2007

Assessment Of Uncertainty In Equivalent Sand Grain Roughness Methods

Chinmay P. Bhatt
University of Alabama at Birmingham

ASSESSMENT OF UNCERTAINTY IN EQUIVALENT SAND GRAIN ROUGHNESS METHODS

by

CHINMAY P BHATT

STEPHEN T. MCCLAIN, COMMITTEE CHAIR

PETER M. WALSH

ROY P. KOOMULLIL

A THESIS

Submitted to the graduate faculty of The University of Alabama at Birmingham,
in partial fulfillment of the requirements for the degree of
Master of Science in Mechanical Engineering

BIRMINGHAM, ALABAMA

2007

ASSESMENT OF UNCERTAINTY IN EQUIVALENT SAND GRAIN ROUGHNESS METHODS

CHINMAY P BHATT

ABSTRACT

The equivalent sand-grain roughness model is an empirical model initiated by Schlichting for predicting skin friction and heat transfer for turbulent flows over rough surfaces. For the equivalent sand-grain roughness model, rough surfaces with various features are compared to data from Nikuradse concerning flow in pipes with varying sizes of sieved sand glued to wetted surface. Rough surfaces are assigned a value of equivalent sand-grain roughness height based on comparisons with Nikuradse's fully rough data. Recent literature on the equivalent sand-grain roughness method has involved seeking correlations for equivalent sand-grain roughness height based on roughness metrics such as height, density and shape. The Sigal-Danberg parameter has demonstrated the most promise for correlating the available equivalent roughness height data to geometric surface information. The Sigal-Danberg parameter was recently modified to include the mean surface elevation as an important parameter. While the modified Sigal-Danberg parameter provides a unified correlation for the equivalent sand-grain roughness height, the new formulation does not improve the scatter of the experimental data around the correlation. An uncertainty analysis is presented to evaluate the uncertainty of equivalent sand-grain roughness height predictions using the unified correlation. The analysis begins by estimating the uncertainties in the experimental measurements of Schlichting, and the uncertainty propagation is evaluated through each step of the equivalent sand-grain method development. The uncertainty associated with using equivalent sand-grain roughness heights in empirical equations for skin friction coefficients as a predictive approach is also discussed. The result is an improved understanding of the uncertainty in skin friction predictions made using the equivalent sand-grain roughness methods.

ACKNOWLEDGMENTS

I would like to take this opportunity to thank those people without whom this research effort wouldn't have been possible. First and foremost I would like to thank my parents for their immense support and encouragement during my higher studies. Their love has always been a source of succor throughout. I will always be indebted to them for the sacrifice they have made for me. I am grateful to my advisor, Dr. Stephen T McClain for guiding me through this often grueling world of research. This valuable feedback helped me shape my research skills. I would also like to thank my committee members, for their precious advice and efforts that greatly contributed to this research work. My friends here at University of Alabama at Birmingham and back home have helped me in all possible ways. I will always be indebted to them.

TABLE OF CONTENTS

APPENDICES

LIST OF TABLES

Table *Page*

LIST OF FIGURES

Figure *Page*

LIST OF ABBREVIATIONS

A_f = roughness element frontal area

A_s = roughness element windward wetted surface area

b = channel test section height

k = roughness height

k_s = equivalent sand grain roughness height

Λ_s = Sigal and Danberg roughness parameter

Λ_{eff} = Modified Sigal and Danberg roughness parameter

Re_k = roughness Reynolds number

S = rough surface flat reference area

S_f = total roughness frontal area

S_s = total roughness windward wetted surface area

x = Distance from the leading edge in the flow direction

W = channel test section spanwise width

ν = kinematic viscosity

τ = surface shear stress

ρ = static density

A = Intercept

u = Average velocity

u_{rc} = Roughness corrected velocity

Y = Distance from the wall

ΔY = Wall shift

- Subscripts

r = rough

s = smooth

c= corrected

meas= measured

eff = effective

av = average

CHAPTER-1

INTRODUCTION

The overall efficiency of any equipment that involves movement of working fluid is dependent on energy losses due to the relative movement of the fluid past the various surfaces of the components. The examples can be given as gas turbine engines, steam turbines, compressors, heat exchangers, piping networks, ships, submarines, aircraft, missiles, re-entry vehicles etc.

These energy losses are due to friction and heat transfer. Depending on the machinery there can be several parameters affecting the skin friction and heat transfer. For instance, in predicting the turbine airfoil metal temperature, the factors affecting accurate prediction could be free-stream turbulence, pressure distribution along the airfoil surface curvature, local metal temperature distribution, laminar to turbulent flow transition and surface roughness.

These losses can be either favorable or detrimental based on application. For example for aircrafts, ships and external portion of turbine, aerodynamic losses and thermal loading are unfavorable and should be as low as possible. However for internal cooling passages of turbine airfoils, increased heat transfer is beneficial so naturally-occurring or manufactured customized surface roughness are widely used.

Among the parameters described above, surface roughness increases both the friction factors and the local heat transfer coefficients. The focus of this study is on the assessment of uncertainty in some of the most widely used equations to predict the heat transfer and skin friction augmentation caused by surface roughness.

1.1 Brief history

Two models have been widely used for the evaluation of the effect of the surface roughness on skin friction and heat transfer. First is the 'equivalent sand grain roughness model' and second is the 'discrete-element model'. The equivalent sand grain roughness model was proposed by Schlichting [1] and is an empirical model in which rough surfaces with various shapes of roughness elements are compared to data from Nikuradse [2] regarding flow in pipe with varying size of sieved sand glued to the surface. The equivalent sand grain roughness height for a specific surface is assigned based on the comparison of the velocity profile with profiles from Nikuradse's surface.

The discrete-element model was also described briefly by Schlichting [1] where he suggests that the total drag on rough surface is the sum of the skin friction from the smooth part and the pressure drag from each roughness elements. The discrete-element model is a semi-empirical model in a sense that it takes into account the physical characteristics of roughness elements in the solution of the boundary layer equations. The basic idea is to apply the two-dimensional, time averaged turbulent boundary layer equations below the crest of roughness elements, considering the reduced flow area and the drag and heat transfer from roughness elements.

1.2 Objective of the study

The equivalent sand-grain surface roughness model has been widely used for variety of numerical prediction codes, as well as for many empirical correlations which are based on experimental data. While the method is widely used, uncertainties in predictions based on the method have not been assessed.

Coleman et al. [3] re-evaluated Schlicting's [1] surface roughness experiments and gave the corrected values for skin friction coefficient and equivalent sand-grain roughness height. They showed that original skin friction coefficients are higher than corrected values by amounts ranging from 0.5 to 73 percent and original equivalent sand-grain roughness values are higher by 26 to 555 percent.

Sigal and Danberg [4] made important advances in accounting for these roughness geometry considerations for uniformly-shaped roughness elements spread in uniform pattern over a test surface and they define roughness parameter called as 'Sigal-

Danberg parameter’. This parameter was again modified by McClain at el. [5] using the mean elevation as an important parameter.

The objective of this study is to perform an uncertainty analysis of these re-evaluated and modified parameters and to determine the uncertainty in predicting skin friction and heat transfer with the use of widely used skin friction correlations. The objectives are summarized below.

- Assess the uncertainties in Schlichting’s experiments
- Assess the uncertainty in the techniques described by Coleman et al. [3] to determine the equivalent sand-grain roughness height
- Assessment of uncertainty in the correlations given by McClain et al. [5] for ‘Modified Sigal-Danberg parameter’ to determine the equivalent sand-grain roughness height
- Assessment of uncertainty in the correlations for skin friction (such as from white [6])

The results of the study will enable a better comparison of the capabilities of the different techniques used to predict skin friction and heat transfer of flows over rough surfaces.

CHAPTER-2

BACKGROUND

2.1 Classical Studies

As stated in the previous chapter, two models are widely used in prediction of surface roughness effects on skin friction and heat transfer. In this chapter a technical and formal background of the equivalent sand-grain roughness model is presented.

The first significant study of roughness was done by Nikuradse [1]. Nikuradse [1] measured the drop in pressure along the pipe length ‘l’ roughened with ‘Goettingen’ sand; the sizes of the grain was varied by using different pipe radius (r), and roughness heights (k), to produce varying radius to height ratios, $\left(r/k \right)$, ranging from 15 to 507. The results were plotted in a graph as shown in Figure-1, which shows the effects of roughness and Reynolds number on friction factor.

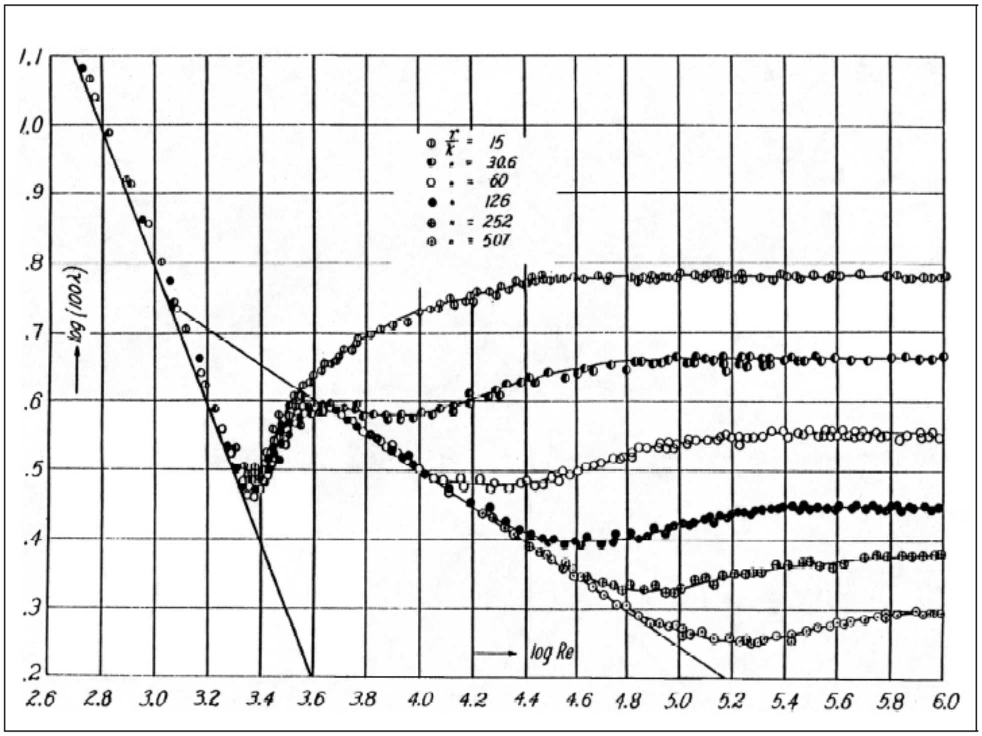

Figure 1. Nikuradse's data of Friction factor vs. Reynolds number [2]

Nikuradse [1] made certain important observations from his study. First, he devised the concept of three different regions of flow over rough surfaces based on roughness Reynolds number (Re_k). First was the "hydraulically smooth" region in which the thickness of the boundary layer is greater than the average roughness projection and therefore the energy losses due to roughness are no greater than those for the smooth pipe, for this region $Re_k<5$.

In the second range the thickness of the boundary layer decreases with increasing Re_k, which causes growing number of individual roughness projections to passes through the boundary layer and increase the energy losses by forming vortices. This range is called 'transition" range. For this region $5< Re_k <70$.

Finally, in the third range (for which Re_k>70), the thickness of the laminar viscous sub- layer has become so small that all the roughness elements extend through it. The energy loss due to the vortices attains a constant value and an increase in Re_k has no effect on resistance. This range is called “Completely rough” region.

From the standpoint of this study, one more observation from Nikuradse’s study requires mentioning. Nikuradse [2] measured velocity profiles for fully rough regime and gave the equation,

$$\frac{u}{u^*} = 5.75 \log({}^{y}\!/_{k_s}) + 8.48 \qquad (2.1)$$

Where, u = mean velocity, u^* = friction velocity, y = distance from the wall, and k_s = equivalent sand-grain height, to describe the velocity profile in the “log” region of the turbulent boundary layer.

2.2 Equivalent sand-grain roughness concept

The next important study in the field of surface roughness was performed by Schlichting [1]. The results and analyses reported by Schlichting [1] have been widely referenced by later workers in the area. Schlichting [1] determined the skin friction for number of surfaces that were roughened with elements of various shapes, sizes and spacing. Schlichting [1], using his measurements was the first one to propose the concept of “Equivalent sand-grain roughness” (k_s). Equivalent sand-grain roughness is actually the size of sand-grain in Nikuradse's [2] experiment, which would give the same resistance as the particular roughness being investigated.

To evaluate k_s Schlichting [1] assumed a constant slope for the logarithmic region for smooth and rough surface. This function can be presented as,

$$\frac{u}{V_g} = 5.5 + 5.75 \log \frac{V_g y}{\nu} \qquad (2.2)$$

Or generalizing the intercept

$$\frac{u}{u^*} = A + 5.75 \log \frac{y}{k} \qquad (2.3)$$

The constant 'A' in later equation denotes intercept and its value changes for each rough surface, and V_g in earlier equation is the shear stress velocity at smooth wall. Schlichting further equated the Nikuradse's equation with his and presented the basis for calculating the Equivalent sand-grain roughness height,

$$\frac{k_s}{k} = e^{\frac{(8.48 - A)}{5.75}} \qquad (2.4)$$

The equivalent sand-grain roughness heights were found by plotting u/u^* versus $\log(y/k)$ for each surface and evaluating the value of the intercept A. Equation (2.4) is then used to evaluate $\frac{k_s}{k}$.

Schlichting [1] showed that the equivalent sand-grain roughness height was not only affected by the height of roughness but also by its shape and density. Other researchers continued to evaluate the velocity profiles and equivalent sand-grain roughness height; the later work involved the use of parameters like roughness shape and density. Dvorak [7], Simpson [8], Dirling [9] and Denman [10] can be considered the significant effort in that direction but Sigal and Danberg [4] made important advances in accounting for these roughness geometry considerations for uniformly-shaped roughness elements spread in a uniform pattern over a test surface. The authors defined a roughness parameter, Λ_s. This parameter actually defines the surface geometry of the rough surface attributable to the use of particular roughness. And by the use of this parameter it was possible to capture the experimental data of equivalent sand grain roughness height in a correlation. The Λ_s can be defined as,

$$\Lambda_s = \left(\frac{S}{S_f}\right)\left(\frac{A_f}{A_s}\right)^{-1.6} \tag{2.5}$$

Where S is the reference area, or the area of the smooth surface before adding on the roughness, S_f is the total frontal area over the rough surface, A_f is the frontal area of a single roughness element, and A_s is the windward wetted surface area of a single roughness element. The (S/S_f) ratio is then a roughness density parameter and the ratio (A_f/A_s) is a roughness shape parameter. The ratio of equivalent sand-grain roughness-to-roughness height, k_s/k, for different ranges of Λ_s as provided by Sigal and Danberg [4],

$$\frac{k_s}{k} = \begin{cases} 0.00321\,\Lambda_s^{4.925} & 1.400 \le \Lambda_s \le 4.890 \\ 8 & 4.890 \le \Lambda_s \le 13.25 \\ 151.71\,\Lambda_s^{-1.1379} & 13.25 \le \Lambda_s \le 100.0 \end{cases} \tag{2.6}$$

Figure-2 provides a good example of irregular and randomly rough surface.

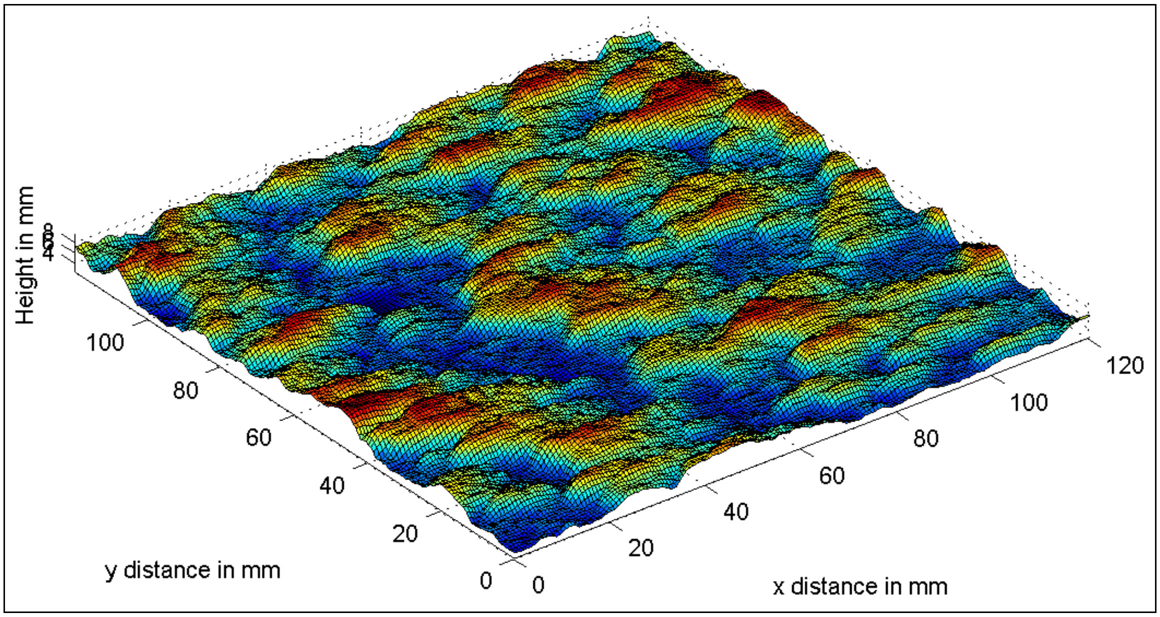

Fig.2. Irregular and randomly rough surface

2.3 Recent Studies

To this point, the studies that were pioneer in their respective approach have been presented. Some recent studies discussed below are either re-evaluation of old studies or give more insight and new parameters to be considered for more accurate prediction of skin friction and heat transfer.

A study conducted by Coleman at el. [3], authors re-evaluated the results of the Schlichting's [1] original data for the surface roughened with spheres, spherical segments and cones. They showed that the original skin friction coefficients were higher than corrected values by 0.5 to 73 percent. Equivalent sand-grain height values were also re-evaluated and it was shown that original values were higher than corrected values by amount ranging from 26 to 555 percent.

Coleman et al. [3] questioned some of the assumptions made by Schlichting. For C_f calculations Schlichting assumed the shear in the smooth side walls to be negligible. While re-evaluating his study Coleman et al. [3] included the side wall shear and gave the modified equation for calculating corrected friction velocities based only on the bulk pressure gradient in the channel,

$$u_{rc}^{*} = \frac{b}{\rho}\left|\frac{dp}{dx}\right| - \left(\frac{W+2b}{1.10W}\right)u^{*}_{s,meas} \qquad (2.7)$$

Where u_{rc}^{*} = roughness corrected velocity, $u^{*}_{s,meas}$ = measured velocity, b = test channel height, W = test channel width. Similarly, the calculations for the Equivalent sand roughness were re-evaluated with the use of corrected values of friction velocities. The method used for correcting Equivalent sand roughness height values follows,

For each surface tested by Schlichting [1], he determined the k_s values and he did this by comparing the rough wall 'log law' in the form

$$\frac{u}{u_{r,av}^{*}} = 5.75\log\left(\frac{y}{k}\right) + A \qquad (2.8)$$

to the Nikuradse's velocity profile data for fully rough regime,

$$\frac{u}{u^*} = 5.75 \log(y/k_s) + 8.48 \qquad (2.9)$$

But it should be noted that in (2.8)

$$y = y' - \Delta y \qquad (2.10)$$

Where y ’is distance from the wall, Δy is wall shift and $u_{r,av}^*$ is average mean velocity. Nikuradse [2] didn’t explicitly define the origin of his y coordinate in equation (2.9). Schlichting set equation (2.8) and equation (2.9) equal with assumption that all his data were in fully rough regime and obtained.

$$5.75 \log(k_s/k) = 8.48 - A \qquad (2.11)$$

By computing the value of intercept ‘A’ from equation (2.8) for a velocity profile and then calculating mean value of intercept ‘A’ from all the profiles on each plate, he was able to use (2.11) to obtain the values of k_s/k. In the view of Coleman et al. [3] the use of $u_{r,av}^*$ and Δy are open to serious question. According to Coleman et al. [3] it is more appropriate to use the corrected friction velocity and wall shift Δz such that,

$$\frac{u}{u_{rc}^*} = 5.75 \log(y' - \Delta y)/k + A \qquad (2.12)$$

If (2.12) is used in determining an equivalent sand-grain roughness then Δy values must be known a priori, for getting this values Coleman et al. [3] used the method from Monin and Yaglom [11]. They showed that within the logarithmic region, the quantity

$$y_0 = (y' - \Delta y) \exp(-\kappa u/u^*) \qquad (2.13)$$

is independent of the distance from the wall. Thus if the friction velocity and the data pairs $(u, y^{'})$ in a velocity profile are known, y_0 can be determined as a function of $(y^{'} - \Delta y)$ for various Δy values. [The optimum Δy value is than one that gives values of z_0 which are closest to being constant.]

The optimum Δy values were determined in Coleman et al. [3] using above approach and setting the Karman constant 'κ' to be 0.40. For each of the profiles for which Δy was calculated, a linear least squares regression of form (2.12) was used to determine the values of 'A'. Then (2.11) was used to calculate the corresponding k_s/k values. Through this correlation, the Equivalent sand-grain roughness values were corrected and corrected values were found to be much less than values originally reported by Schlichting.

One more study of note is by McClain et al. [5], in which authors have suggested to use the mean elevation as the reference. The authors have modified the equivalent sand-grain roughness height (k_{eff}) & sigal-denberg parameter (Λ_{eff}) on the basis of mean elevation. The concept of mean elevation can be shown by Figure 3.

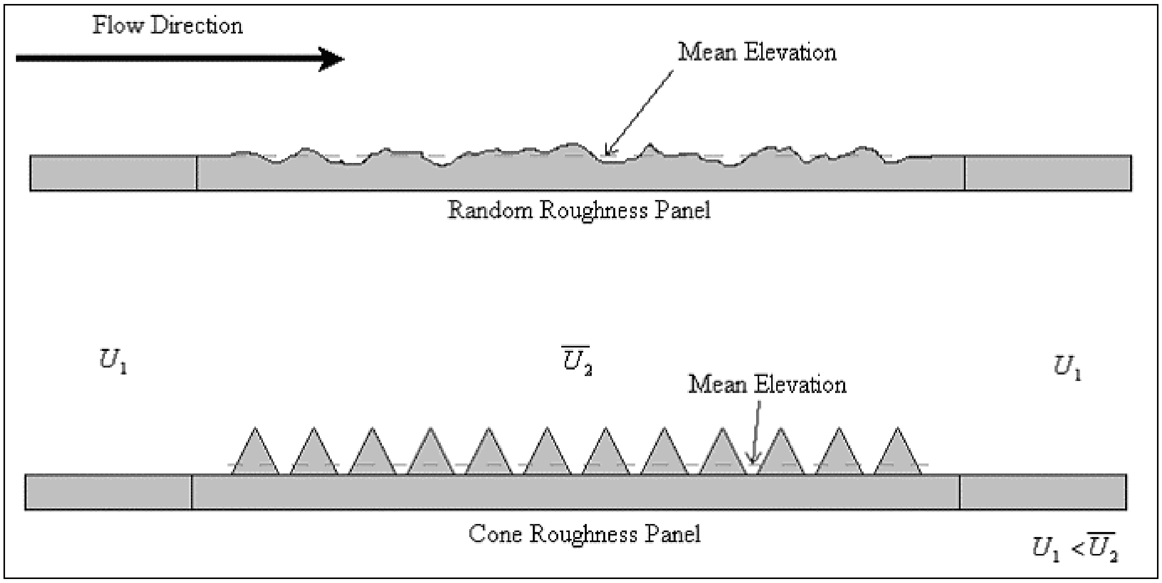

Figure 3. The mean elevation for randomly rough and cone roughness panel [5]

This study is important in demonstrating why maximum equivalent sand-grain roughness height does not occur at the most dense spacing but at considerably larger spacing. To explain this, consider the Figure 4 with and without taking mean elevation as the no-slip plane.

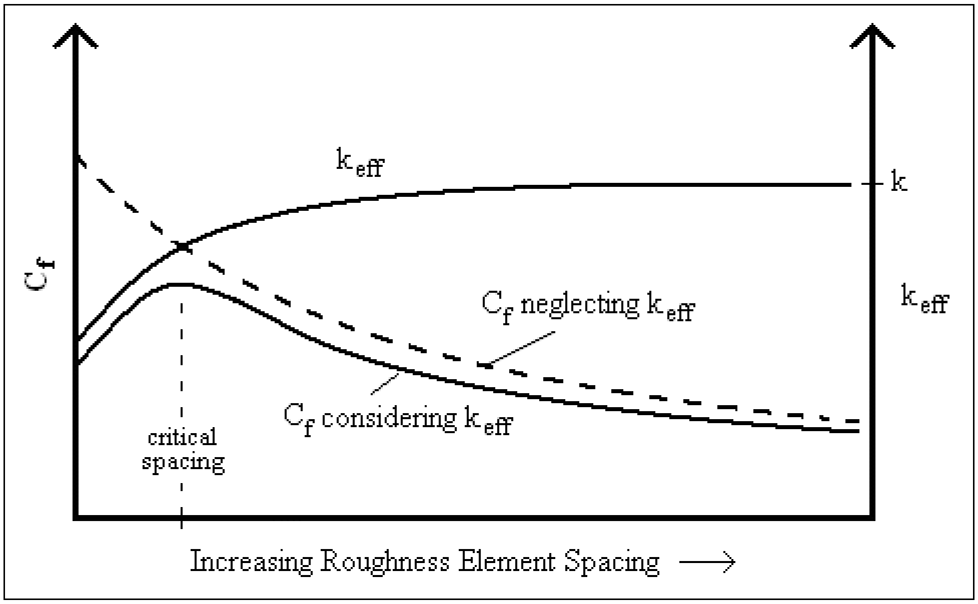

Fig.4. Change in Skin Friction coefficient and Effective roughness heights as function of Roughness Spacing [5]

This figure indicates why the critical spacing does not occurr at the maximum density of roughness elements and explains the observation Schlichting made in his study. McClain et al. [5] gives the correlation for $\left({k_s}/{k_{eff}}\right)$ & $\left(\Lambda_{eff}\right)$ as follows,

$$\left({k_s}/{k_{eff}}\right) = 927.317\left(\Lambda_{eff}\right)^{-1.669} \qquad (2.14)$$

Where,

k_{eff} = effective roughness height, Λ_{eff} = modified Sigal-Danberg parameter

To completely understand the objective of this study some basic idea about uncertainty is also important, abridged description of uncertainty analysis follows.

2.4 Uncertainty

The word ‘uncertainty’ appeared several times in this paper, the basic idea of uncertainty follows.

2.4.1 The Concept of Uncertainty

No measurement is perfectly accurate and thus means for describing inaccuracies are required. An uncertainty is not same as error, error in measurement is the difference between the true and recorded value. In this sense an error is a fixed number and not a statistical variable. An ‘uncertainty’ is a possible value that the error might take on various values for a range of readings. It is inherently a statistical variable.

Some important definitions in uncertainty analysis follow. Accuracy refers to the closeness of agreement between a measured value and true value. Total measurement error is the difference between the measured value and the true value. The total error is the sum of systematic (or bias) error and random (or precision) error. The systematic (or bias) error is the fixed or constant component of the total error and is sometimes referred as the bias. The random component of the total error is sometimes called the repeatability, repeatability error, or precision error.

2.4.2 General equations for Uncertainty Analysis

Considering a case in which an experimental result, *r*, is function of *J* measured variables X_i.

$$r = r\,(X_1, X_2, \ldots, X_J) \qquad (2.15)$$

The above given equation *(a)* is the data reduction equation used for determining *r* from measured values of the variables X_i. Then, neglecting situations when the uncertainties of the measured variables are dependent on one another, the uncertainty in the results is given by,

$$U_r^2 = \left(\frac{\partial r}{\partial X_1}\right) U_{X_1}^2 + \left(\frac{\partial r}{\partial X_2}\right) U_{X_2}^2 + \ldots + \left(\frac{\partial r}{\partial X_J}\right) U_{X_J}^2 \qquad (2.16)$$

In equation (2.16), U_{X_i} are the uncertainties in the measured variable X_i.

CHAPTER-3

PROCEDURE

The main objective of this of this study is to evaluate the uncertainties within the correlations for equivalent sand-grain roughness height and subsequently skin friction coefficient. In this chapter, the methods to quantify the uncertainties associated with each step of equivalent sand-grain roughness procedure are detailed.

Equivalent sand-grain roughness height values are obtained either by experimental data or by using correlations given by Sigal and Danberg [4] or McClain et al. [5]. However, these correlations also depend on the experimental data. Hence the first step towards the objective is to calculate the uncertainty present in the experimental data.

In the experimental equivalent sand-grain roughness evaluations, Schlichting first made measurements of the velocity profile for flows over rough surfaces. The velocity profile points were then used to determine the "Law of the Wall" intercept offset, *A*, from

Equation (2.8). Equation (2.4) was then used to determine the equivalent sand-grain roughness height.

To evaluate the uncertainty associated with the equivalent sand-grain roughness height experiments, the uncertainty in the experimental methods used by Schlichting must be evaluated beginning with the velocity profiles. Unfortunately, many of the basic measurements made by Schlichting were not reported in tabulated form. The following sections identify how the measured profile data points were extracted, how extracted measurements were used to determine the equivalent sand-grain roughness heights, and how uncertainty is propagated through each step of the equivalent sand-grain roughness experimental measurements. The last sections of this chapter identify how the uncertainties propagate through the correlation of McClain et al. [5] and through skin friction predictions based on equivalent sand-grain heights produced by this correlation.

3.1 Calculation of the data

To determine the uncertainty in the intercept, *A*, it was necessary to find out the uncertainties in the each of the quantities of the equation (3.1). This includes finding out uncertainties of velocity (u), roughness velocity (u_{rc}), distance from the wall (y), and wall shift (Δy). The section is divided in four major parts. The first part will be the collection of data needed to place in the Equation (3.1), the second part will be the uncertainty analysis of the quantities involved in equation (3.1), the third part is to calculate of uncertainty in the intercept 'A' and equivalent sand-grain height equations, and finally, the fourth part is a sample calculation illustrating the uncertainty propagation through skin friction predictions.

All the information needed to evaluate the intercept was in the form of the graph, the following procedure describes the calculations made in order to calculate all the parameters needed to calculate the intercept, *A*. Later in the section, the calculation of the intercept is also illustrated.

3.1.1 Determining average velocity (u) & distance from wall (y)

The first step was to evaluate the average velocity and distance from the wall from the Schlichting's data. However the data was only available in the form of graphs of $\frac{u}{v_* r}$ vs. $\log\frac{y}{k}$ as shown in Fig. 5. Hence the graphs were first scanned with 300 dpi resolutions and than the values were obtained by a multivariable regression formula incorporating 'loess' and 'interp' function in MathCAD which will give X &Y coordinate values by identifying the pixel values for any given point on the graph. The Fig. 5 shows the velocity profile data that Schlichting gave in his study, five different lines indicates five different plates. For each plate six different velocity profiles are presented as it can be seen from in the top of the graph.

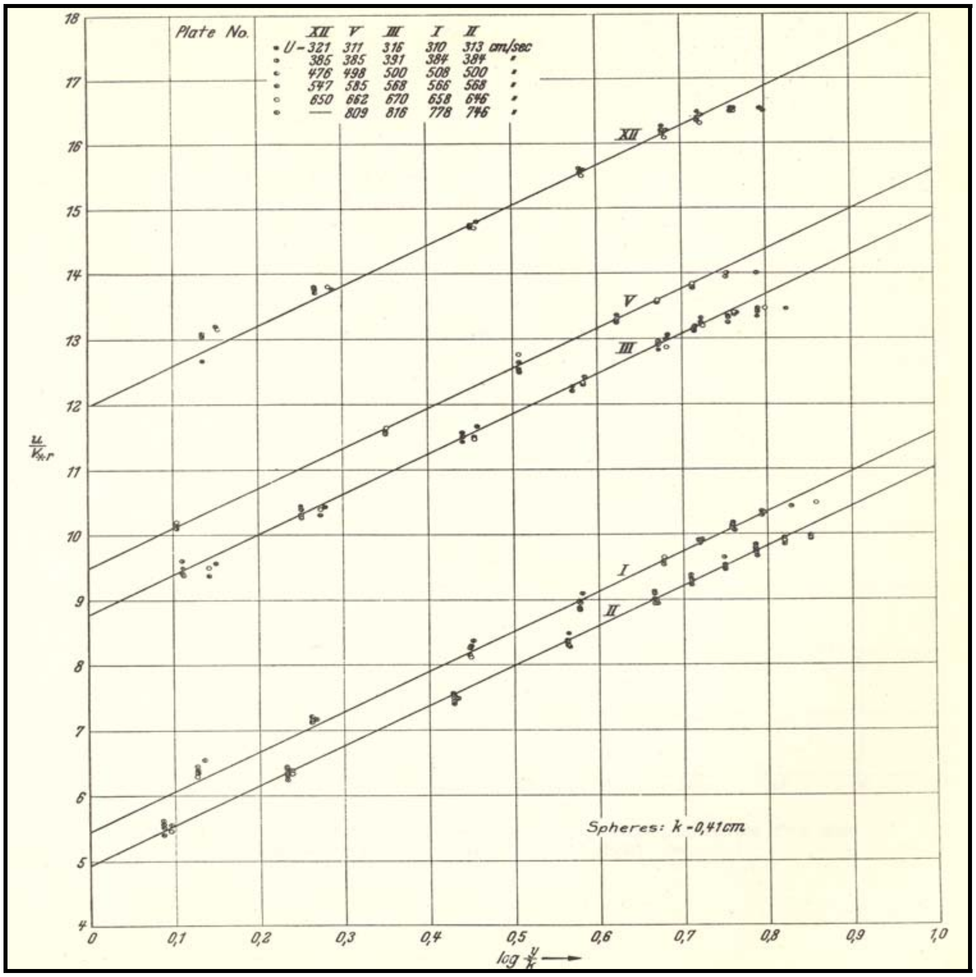

Figure 5. Nondimensional velocity distribution for spherical roughness, k=0.41 cm [1]

After obtaining the values of X &Y coordinate, which is basically $\log\frac{y}{k}$ and $\frac{u}{v_* r}$ respectively, the values of velocity (u) and distance from the wall (y) were calculated by following correlations ,

$$Y = k.10^{\log y/k} \tag{3.1}$$

and

$$u = \frac{u}{v_* r}.v_* r \tag{3.2}$$

Where, $v_* r$ = shear stress velocity at rough wall. The example calculation is provided in Appendix-A.

3.1.2 Determining friction velocity

After calculating average velocity (u) & distance from wall (y), the corrected friction velocities were calculated following Equation.

$$u_{rc}^{\ *} = \sqrt{\frac{b}{\rho}\left|\frac{dp}{dx}\right| - \left(\frac{W + 2b}{1.10W}\right) u^{*}_{s,meas}} \tag{3.3}$$

By substituting the values of width (w), height (b) and measured velocity ($u^{*}_{s,meas}$) from Schlichting's data, the friction velocity was calculated. Appendix-B presents detailed example calculation.

3.1.3 Determining wall shift

The concept of the wall shift (Δz) was discussed in the previous chapter. To calculate the wall shift the standard uncertainty analysis equation for slope (M) was used,

$$M = \frac{N\sum_{j=0}^{N-1}(X_j Y_j) - \sum_{j=0}^{N-1}(X_j)\sum_{j=0}^{N-1}(Y_j)}{N\sum_{j=0}^{N-1}(X_j)^2 - (\sum_{j=0}^{N-1} X_j)^2} \tag{3.4}$$

In this equation the X is,

$$X = (z - \Delta z) \qquad (3.5)$$

And Y is,

$$Y = (z' - \Delta z)\exp\left(-\kappa u / u_*\right) \qquad (3.6)$$

The wall shift was calculated for each of the profile using the slope equation given above. A MathCAD "Given-Find" solve block was used to find the wall shift that forces the slope M to be zero. The sample calculation for cone surface profiles can be found in Appendix-C.

3.1.4 Calculating the Intercept 'A'

After the calculating quantities like velocity (u), distance from the wall (y), wall shift (Δz or Δy) and friction velocity; the intercept 'A' was calculated for each profile by,

$$A = \frac{u}{u_{rc}} - 5.75.\log\left(\frac{y - \Delta y}{k}\right) \qquad (3.7)$$

And after calculating 'A' for each profile, the average 'A' for the whole plate was calculated. This process was done for all the plates in the study. A detailed calculation is presented in Appendix-D.

3.2 Calculation of the uncertainty

This section evaluates the uncertainty of the individual quantities that forms equation (2.8), followed by uncertainty in the intercept 'A'.

3.2.1 Determining uncertainty of velocity (u)

To find out the uncertainty in the velocity following equation was used as the data reduction equation for schlichting's experiments.

$$u = \sqrt{2 g \Delta h_p} \tag{3.8}$$

In the equation the Δh_p term is the difference in manometer height, the uncertainty assumption for this parameter is given in Table (3.1). And after calculating Δh_p the equation was differentiated in the form described below to calculate the uncertainty of velocity (U_u).

$$U_u = \frac{\partial u}{\partial \Delta h} U_{\Delta h} \tag{3.9}$$

With this equation the uncertainty was calculated. An example calculation is given in Appendix-E with details.

3.2.2 Determining uncertainty of distance from the wall (y)

The uncertainty for the distance was assumed to be 0.1mm. This was based on the assumed method for measuring the height which was most likely a micrometer screw.

3.2.3 Determining uncertainty of the friction velocity

Equation (2.7) was used as the data reduction equation. Where u_{rc}^{*} denotes the friction velocity. For calculation of the uncertainty, it was necessary to evaluate the uncertainties of the pressure difference term $\frac{b}{\rho}\left|\frac{dp}{dx}\right|$, measured velocity $u^{*}_{s,meas}$, w and b. Appropriate assumptions were made for the uncertainties of the measured velocity, w and b. For the calculation of the pressure difference term, the following data reduction equation which was derived from the Bernoulli's equation,

$$\frac{1}{\rho}.\frac{dp}{dx} = g.\frac{\Delta h_s}{\Delta x} \tag{3.10}$$

Where,

Δh_s = Static pressure manometer height difference

$\Delta x =$ Distance between manometer connections

The following Table (3.1) explains the bases of uncertainty assumptions for some of the parameters used in previous equations. After calculating the all the measurement uncertainties, equation (3.5) was used to calculate the uncertainty of the friction velocity. A detailed calculation is given in Appendix-F

Table 1. Basis of Uncertainty assumptions

Measured variable	**Equation**	**Uncertainty**	**Remarks**
Δh	3.10	2 mm	Assuming to be measured with scale
Δx	3.10	1 mm	Assuming to be measured with scale
Δh (Pitot)	3.8	1/100 inch	Assumed to be measured with slanted manometer
$u^{*}{}_{s,meas}$	2.7	5%	Assuming standard uncertainty due to lack of information

3.2.4 Determining uncertainty of the wall shift

No simple method was available to calculate the uncertainties in the wall shift. Hence the brute force method was applied to find out the uncertainties. In this method the equation (3.6) was used. In this equation the X and Y were added its individual uncertainty ΔX and ΔY then the database was created with the difference in the final wall shift value change and than basic definition of finite derivative which

$$\frac{dX}{dY} = \frac{X_1 - X_2}{\Delta Y} \tag{3.11}$$

This equation was used, and then after differentiating each of the quantities, the uncertainty analysis equation was used to find out the uncertainty of wall shift in that profile. This was done for each of the profile. The detailed calculations are explained in detail in the Appendix-G

3.2.5 Determining uncertainty of the intercept

After obtaining all the values and uncertainties used in Equation (3.1), it is now possible to calculate the uncertainty of intercept ‘A’ using Equation (3.1) as the data reduction equation.

$$A = \frac{u}{u_{rc}} - 5.75\log(\frac{Y - \Delta Y}{k}) \tag{3.12}$$

After getting the uncertainty of ‘A’ for each profile, the average uncertainty was calculated. The detailed calculation is shown in Appendix H.

3.3 Equivalent sand-grain height Uncertainty evaluation

This section shows the calculation for evaluating uncertainty in Schlichting’s measurements followed by assessment of uncertainty in equivalent sand grain roughness height correlations by McClain at al. [5].

3.3.1 Determining Uncertainty of K_s / K

After obtaining the uncertainty in intercept, A, the next step was to find out the uncertainty in the $\frac{k_s}{k}$ values. The following equation is used as the data reduction equation,

$$\frac{k_s}{k} = e^{\frac{(8.48 - A)}{5.75}} \tag{3.13}$$

After differentiating this equation following equation was used for finding out the uncertainty,

$$U_{k_s/k} = \frac{\partial k_s/k}{\partial A} U_A \tag{3.14}$$

And after substituting the values in this equation the uncertainty in k_s/k values were obtained. Refer to Appendix H for detailed calculations.

3.3.2 Determining Uncertainty of the k_s/k_{eff}

After obtaining the uncertainty values of k_s/k, the following equation was used to find the uncertainty of k_s/k_{eff}.

$$\frac{k_s}{k_{eff}} = \frac{k_s}{k} . \frac{k}{k_{eff}} \tag{3.15}$$

The values of K_{eff} were taken from the data available in tabular form. After differentiating the above given equation the following form was obtained. Then the values were substituted to obtain the uncertainty values,

$$U_{k_s/k_{eff}} = \frac{k}{k_{eff}} U_{k_s/k} \tag{3.16}$$

After substituting the values in this equation the uncertainty of k_s/k_{eff} was evaluated.

A detailed calculation is provided in Appendix H.

3.3.3 Correlation uncertainty bands

After calculating the experimental measurement uncertainties, the uncertainty in predicted $\frac{k_s}{k_{eff}}$ values from the correlation of McClain et al [5] must be evaluated. The correlation equation from McClain et al has the non-linear form:

$$\frac{k_s}{k_{eff}} = 10^b \Lambda_{eff}^p \tag{3.17}$$

Appendix I shows that the correlation method proceeds in two steps. Since the correlation of (3.17) is nonlinear, the experimental measurements must be transformed using

$$Z = \log\left(\frac{k_s}{k_{eff}}\right) \tag{3.18}$$

and

$$W = \log\left(\Lambda_{s,eff}\right) \tag{3.19}$$

Using these transformations, the constants of the correlation, equation (3.17), are evaluated using the linear regression equation

$$Z = pW + b \tag{3.20}$$

Where the constants are evaluated as

$$p = \frac{N\sum_{j=0}^{N-1}(W_j Z_j) - \sum_{j=0}^{N-1}(W_j)\sum_{j=0}^{N-1}(Z_j)}{N\sum_{j=0}^{N-1}(W_j)^2 - (\sum_{j=0}^{N-1}W_j)^2} \tag{3.21}$$

and

$$b = \frac{\sum_{j=0}^{N-1}(W_j)^2 \sum_{j-0}^{N-1} Z_j - \sum_{j=0}^{N-1}(W_j)\sum_{j=0}^{N-1}(W_j Z_j)}{N\sum_{j=0}^{N-1}(W_j)^2 - (\sum_{j=0}^{N-1} W_j)^2} \tag{3.22}$$

Neglecting the measurement of surface geometric measurement uncertainties for a new surface, the uncertainty of a predicted $\frac{k_s}{k_{eff}}$ value based on geometric surface quantities is then

$$U^2_{\left(\frac{k_s}{k_{eff}}\right)_{pred}} = \sum_{i=1}^{N_S}\left(\frac{\partial\left(\frac{k_s}{k_{eff}}\right)_{pred}}{\partial\left(\frac{k_s}{k_{eff}}\right)_{Exp,i}} U_{\left(\frac{k_s}{k_{eff}}\right)_{Exp,i}}\right)^2 + \sum_{i=1}^{N_S}\left(\frac{\partial\left(\frac{k_s}{k_{eff}}\right)_{pred}}{\partial\Lambda_{eff,Exp,i}} U_{\Lambda_{eff,Exp,i}}\right)^2 + \left(\frac{\partial\left(\frac{k_s}{k_{eff}}\right)_{pred}}{\partial Z}(2\cdot SEE)\right)^2 \tag{3.23}$$

Where $\left(\frac{k_s}{k_{eff}}\right)_{pred}$ is the predicted value of relative sand-grain roughness height, $\left(\frac{k_s}{k_{eff}}\right)_{Exp,i}$ represents each experimentally measured value of the relative sand-grain roughness height based on Schlichting's measurements, $\Lambda_{eff,Exp,i}$ represents the modified Sigal-Danberg values for each of the surfaces of Schlichting, N_S is the number of surfaces used in the present study, and *SEE* is the regression line standard error of the estimate.

3.4 Skin friction coefficient uncertainty

Numerous widely used skin friction correlations utilize equivalent sand-grain height values. There could be infinite number of different surfaces and Reynolds numbers of interest; hence it is not feasible to predict the skin friction uncertainties in all of them. Therefore a sample calculation for assessing skin friction uncertainty for flow over a flat plat with cone roughness is provided.

An example skin friction coefficient and uncertainty calculation is provided to enable an understanding of uncertainty propagation when using the modified Sigal-Danberg correlation for equivalent sand-grain roughness height. The example calculation provides uncertainty of skin friction prediction based on the correlation from White [6] for prediction skin friction coefficients for flows over rough flat plates. White's correlation is

$$C_f = \left(1.4 + 3.7\log\left(\frac{x}{k_s}\right)\right)^{-2} \tag{3.24}$$

Where x is the distance from the leading edge of the plate in the flow direction, and k_s is equivalent sand-grain roughness height.

The correlation from McClain at el [5] was used for predicting the equivalent sand-grain roughness height. Then, the uncertainties in predicted equivalent sand-grain roughness height were evaluated using Equation (3.23). Subsequently, the skin friction coefficient was predicted using equation (3.24), and then following equation was used to evaluate the uncertainties in predicted skin friction coefficient.

$$U_{c_f} = \left(\frac{\partial c_f}{\partial k} \right) U_{k_s} \tag{3.25}$$

This calculation represents the uncertainties based only on the predicted equivalent sand-grain roughness value from the modified Sigal-Danberg correlation.

CHAPTER-4

RESULTS AND DISCUSSION

This chapter presents the results of the uncertainty analysis for the experimental measurements of Schlichting [1] as modified by Coleman et al. [3]. The resulting uncertainties for the predicted equivalent sand-grain roughness values (based on the modified Sigal-Danberg) are presented. Finally, an example calculation of the uncertainty in skin friction calculations based on predicted equivalent sand-grain roughness values is discussed.

4.1 Experimental Uncertainties

Table 2 presents the relative equivalent sand-grain roughness measurements from Schlichting [1] (as modified by Coleman et al. [3]) and the resulting measurement uncertainties. The first column in Table 2 below indicates the measurements obtained by Schlichting [1] and second column shows the uncertainty in the measurements. The third column presents the effective relative equivalent sand-grain roughness heights reported by McClain at el [5]. Finally, the fourth column shows the uncertainty in the effective relative equivalent sand-grain roughness heights.

Table 2. Uncertainty Results

Plate No.	**Value of** $\frac{k_s}{k}$	**Uncertainty of** $\frac{k_s}{k}$	**Value of** $\frac{k_s}{k_{eff}}$	**Uncertainty of** $\frac{k_s}{k_{eff}}$
IV	2.47	0.09727	2.72	0.10718
I	2.43	0.06267	2.6645	0.06872
2a Bogard*	3.20	0.0000	3.92	0.00000
II	2.59	0.05231	3.4281	0.06924
V	0.378	0.02832	0.9363	0.07016
XIX	0.953	0.05251	1.983	0.10930
VI	0.43	0.02747	0.4401	0.02812
XXV	0.471	0.021	0.4944	0.02200
III	0.41	0.02317	0.41922	0.02369
2b Bogard*	0.5	0.0000	0.6113	0.00000
1 Bogard*	0.5	0.0000	0.6111	0.00000
XV	0.278	0.00195	0.2994	0.00211
XXIV	0.112	0.01200	0.1246	0.01200
XIV	0.034	0.00452	0.035119	0.00467
XXIII	0.046	0.006093	0.046551	0.00616
XII	0.12	0.00921	0.12066	0.00926
XIII	0.018	0.003305	0.01833	0.003366

(* The data is not evaluated in the present study)

The effective relative equivalent sand-grain roughness heights are plotted in Figure 6 versus the modified Sigal-Danberg parameter. The uncertainty bars for each surface are also included. From Figure 6, the low experimental uncertainties relative to the experimental scatter about the trend is evident

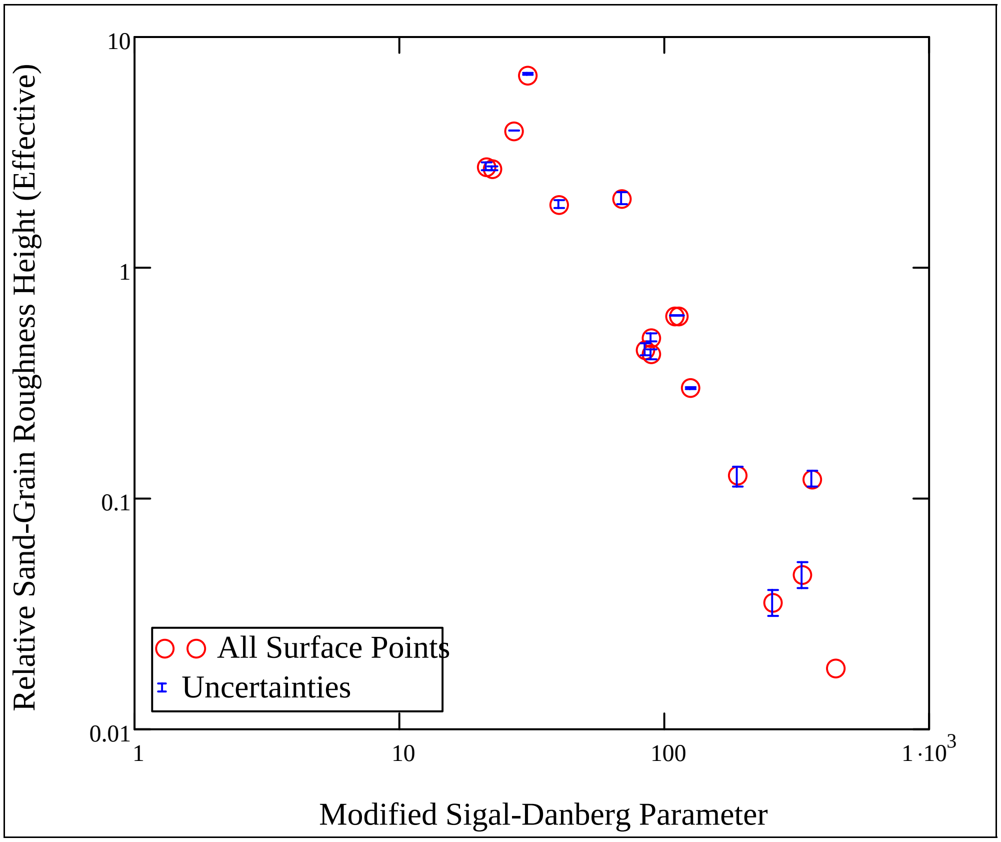

Figure 6. Graph showing k_{eff} vs. Λ_{eff} data points

Figure 7 illustrates the log of effective relative equivalent sand-grain roughness heights versus log of modified Sigal-Danberg parameter with correlation uncertainty bands which capture the scatter of the data. Figure 8 also shows the effective relative equivalent sand-grain roughness heights versus modified Sigal-Danberg parameter with systematic uncertainty bands and experimental uncertainty of each data point. Figure 8 is presented because it is more like the representation of the data in the classical literature.

The detailed regression analysis is provided in Appendix I.

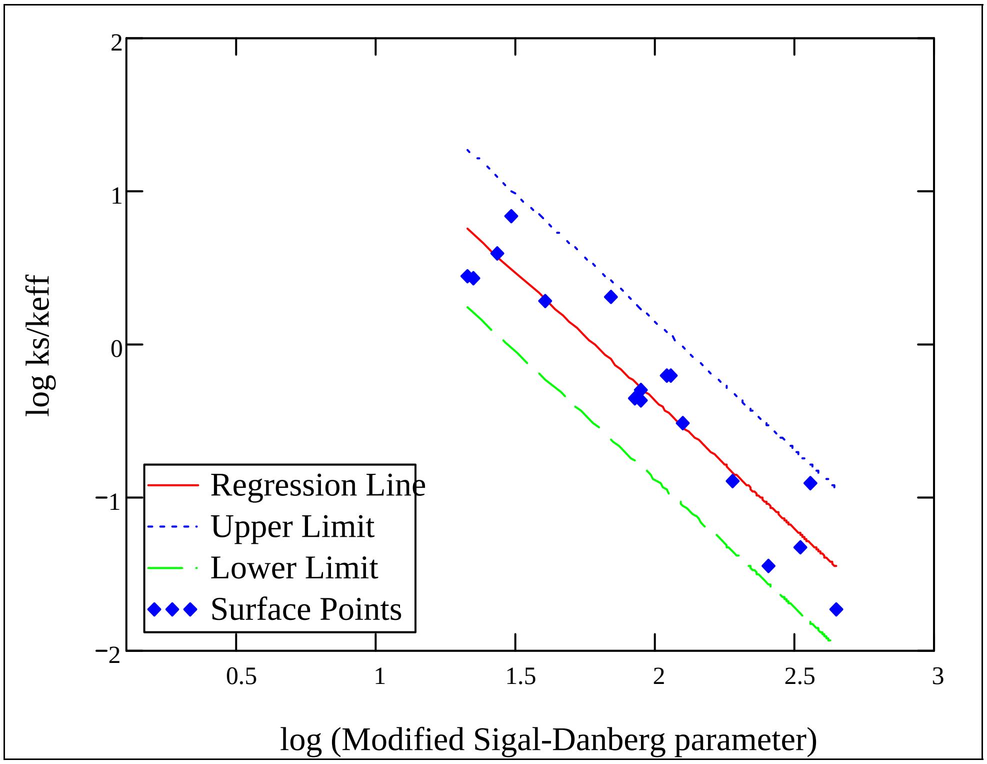

Figure7. log $\frac{k_s}{k_{eff}}$ Vs. log (Λ_{eff}) with systematic uncertainty bands

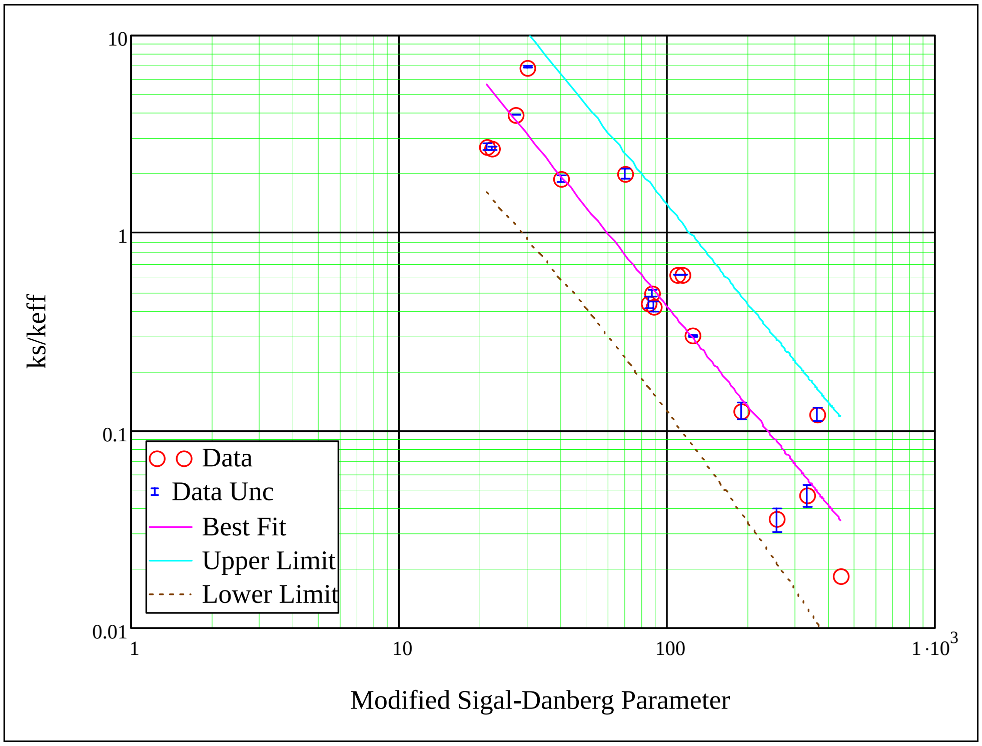

Figure 8. $\frac{k_s}{k_{eff}}$ **Vs.** Λ_{eff} **with uncertainty bands and best fit line**

4.2 The results of the C_f uncertainty

A flow of air at 20 m/s over plate No. XXV of Schlichting's study is used as the example case for skin friction coefficient and uncertainty evaluation. Surface XXV consists of truncated cones. The effective height of the roughness elements above the mean elevation and modified Sigal-Danberg parameters were known for this surface.

For the example calculation, the properties of air such as density and viscosity were taken at 1 atmosphere pressure and 25 °C. To evaluate the distance from the leading edge of the plate, the Reynolds number was taken as 10^6 for turbulent flow. This Reynolds number was chosen because it is approximately four times the Reynolds number at which flow naturally transitions from laminar to turbulent for flow over a flat plate (approximately 250,000).

The detailed skin friction coefficient uncertainty calculation is shown in the Appendix-J. The results showed the upper uncertainty in the predicted skin friction coefficient to be 65.63%, while the lower uncertainty is 20.16% of the predicted value. This calculation demonstrates that when used in a predictive capacity, the equivalent sand-grain roughness method produces skin friction predictions with a very high level of uncertainty.

CHAPTER-5

CONCLUSION

Equivalent sand-grain roughness methods are still widely used for predicting skin friction coefficients. Both experimental and predictive approaches have been developed and re-evaluated over the years. But these methods are used without comprehensive information regarding the uncertainty associated with the equivalent sand-grain height correlations. The uncertainty associated with the equivalent sand-grain height correlations also affects the skin friction coefficient predictions.

In the present study the uncertainty in Schlichting's measurements were assessed. Subsequently the propagation of the uncertainty through predictive sand-grain roughness height approach was evaluated. And finally the uncertainty in skin friction prediction based on predictive method was investigated.

The result shows the uncertainty in the Schlichting's experimental data is not immense, but the correlation used for predicting equivalent sand-grain roughness height magnifies the uncertainty. The chief portion of uncertainty comes from the fact that the data is scattered and hence the correlation is not able to predict the values very accurately. The skin friction coefficient prediction sample calculation shows significant amount of uncertainty in the skin friction coefficient predictions.

Given the high uncertainties in the predicted skin friction coefficient values, a better correlation for predicting the equivalent sand-grain height is required. Future explorations also include (1) evaluating uncertainty in predicting rough surface heat transfer and (2) determining the uncertainties in equivalent sand-grain roughness height predictions as used in CFD ‘wall function’ approaches.

Wall functions basically model the near-wall region using empirical laws to predict a logarithmic velocity profile near a wall. With these laws it is possible to express the mean velocity parallel to the wall and turbulence quantities outside the viscous sub layer in terms of the distance to the wall and wall conditions such as wall shear stress, pressure gradient and wall heat transfer. The uncertainty associated with wall function approaches must be evaluated in a future study.

LIST OF REFERENCE

[1] Schlichting, H., 1936, "Experimental Investigation of the Problem of Surface Roughness," NACA TM-832, National Advisory Committee on Aeronautics.
[2] Nikuradse, J., 1933, "Laws of Flow in Rough Pipes," NACA TM 1292, National Advisory Committee on Aeronautics.
[3] Coleman, H. W., Hodge, B. K., and Taylor, R. P., 1984, "A Re-Evaluation of Schlichting's Surface Roughness Experiment," ASME J. Fluids Eng., 106, pp. 60–65.
[4] Sigal, A. and Danberg, J. E., 1990, "New Correlation of Roughness Density Effect on the Turbulent Boundary Layer," AIAA J., 28, No. 3, pp. 554–556.
[5] McClain, S. T., Collins, S. P., Hodge, B. K., and Bons, J. P., 2006, "The importance of mean elevation in predicting skin friction for flow over closely packed surface roughness," ASME Journal of Fluids Engineering, Vol. 128, pp. 579-586
[6] White, F. M., 1991, Viscous Fluid Flow, 2nd Edition, McGraw-Hill, New York, NY.
[7] Dvorak, F.A., 1969, "Calculation of turbulent boundary layers on rough surfaces in pressure gradients," AIAA journal, Vol. 7 pp. 1752-1759.
[8] Simpson R.L., 1973, "A generalized correlation of roughness density effects on turbulent boundary layer," AIAA Journal, Vol. 11, pp. 242-244.
[9] Dirling, R.B., 1973, "A method for computing rough wall heat transfer rates on reentry nose tips," AIAA paper no. 73-763.
[10] Denman, G.L., 1973, "Turbulent boundary layer rough surface heat transfer on blunt bodies at high heating rates," AIAA paper no. 73-763.
[11] Monin, A.S., and Yaglom, A.M., 1971, Statistical fluid mechanics, Vol. 1, MIT Press.

APPENDIX A

CALCULATING THE VELOCITY (u) AND DISTANCE FROM THE WALL (y)

In order to interpret the values from the scanned graphs, the matrix was created of the reference points for which the x and y co-ordinate values were known. These reference points are shown below with their x and y co-ordinates.

- **Data points for Plate 25, Cone Roughness**

$$A := \begin{pmatrix} 607 & 882 \\ 690 & 883 \\ 771 & 884 \\ 854 & 885 \\ 937 & 885 \\ 1019 & 886 \\ 1101 & 887 \\ 1184 & 887 \\ 1267 & 888 \\ 1348 & 889 \\ 608 & 799 \\ 608 & 715 \\ 609 & 631 \\ 610 & 546 \\ 611 & 461 \\ 612 & 377 \\ 1021 & 635 \\ 1187 & 551 \\ 1188 & 466 \\ 1270 & 467 \\ 772 & 716 \\ 938 & 718 \\ 1103 & 719 \\ 1268 & 721 \\ 774 & 547 \\ 940 & 548 \\ 1105 & 550 \\ 1270 & 551 \\ 776 & 378 \\ 941 & 380 \\ 1106 & 381 \\ 1271 & 382 \end{pmatrix} \qquad X := \begin{pmatrix} 0 \\ 0.1 \\ 0.2 \\ 0.3 \\ 0.4 \\ 0.5 \\ 0.6 \\ 0.7 \\ 0.8 \\ 0.9 \\ 0 \\ 0 \\ 0 \\ 0 \\ 0 \\ 0 \\ 0.5 \\ 0.7 \\ 0.7 \\ 0.8 \\ 0.2 \\ 0.4 \\ 0.6 \\ 0.8 \\ 0.2 \\ 0.4 \\ 0.6 \\ 0.8 \\ 0.2 \\ 0.4 \\ 0.6 \\ 0.8 \end{pmatrix} \qquad Y := \begin{pmatrix} 8 \\ 8 \\ 8 \\ 8 \\ 8 \\ 8 \\ 8 \\ 8 \\ 8 \\ 8 \\ 9 \\ 10 \\ 11 \\ 12 \\ 13 \\ 14 \\ 11 \\ 12 \\ 13 \\ 13 \\ 10 \\ 10 \\ 10 \\ 10 \\ 12 \\ 12 \\ 12 \\ 12 \\ 14 \\ 14 \\ 14 \\ 14 \end{pmatrix}$$

The following equations are used to evaluate the X and Y values from the Graphs

$$X2(x,y) := \mathrm{interp}\left[\mathrm{loess}(A, X, 1), A, X, \begin{pmatrix} x \\ y \end{pmatrix}\right]$$

$$Y2(x,y) := \mathrm{interp}\left[\mathrm{loess}(A, Y, 1), A, Y, \begin{pmatrix} x \\ y \end{pmatrix}\right]$$

- **Calculation:-**

The below given matrix is for the datapoins of the profile points

Datapoints:-

$$PX_2 := \begin{pmatrix} 846 \\ 1004 \\ 1266 \\ 1295 \\ 732 \\ 1005 \\ 1202 \\ 1237 \\ 845 \\ 1114 \\ 1197 \\ 1232 \\ 745 \\ 857 \\ 1120 \\ 1202 \end{pmatrix} \quad PY_2 := \begin{pmatrix} 734 \\ 625 \\ 462 \\ 453 \\ 794 \\ 614 \\ 482 \\ 461 \\ 721 \\ 532 \\ 483 \\ 464 \\ 779 \\ 716 \\ 535 \\ 481 \end{pmatrix} \quad U := \begin{pmatrix} 310 \\ 310 \\ 310 \\ 310 \\ 388 \\ 388 \\ 388 \\ 388 \\ 668 \\ 668 \\ 668 \\ 668 \\ 787 \\ 787 \\ 787 \\ 787 \end{pmatrix} \cdot \frac{cm}{sec}$$

$i := 0..\,\mathrm{rows}(PX_2) - 1 \qquad j := 0..\,3 \qquad k := 4..\,7 \qquad l := 8..\,11 \qquad m := 12..\,15$

$logyk_i := X2\left(PX_{2_i}, PY_{2_i}\right) \qquad ubyv_i := Y2\left(PX_{2_i}, PY_{2_i}\right)$

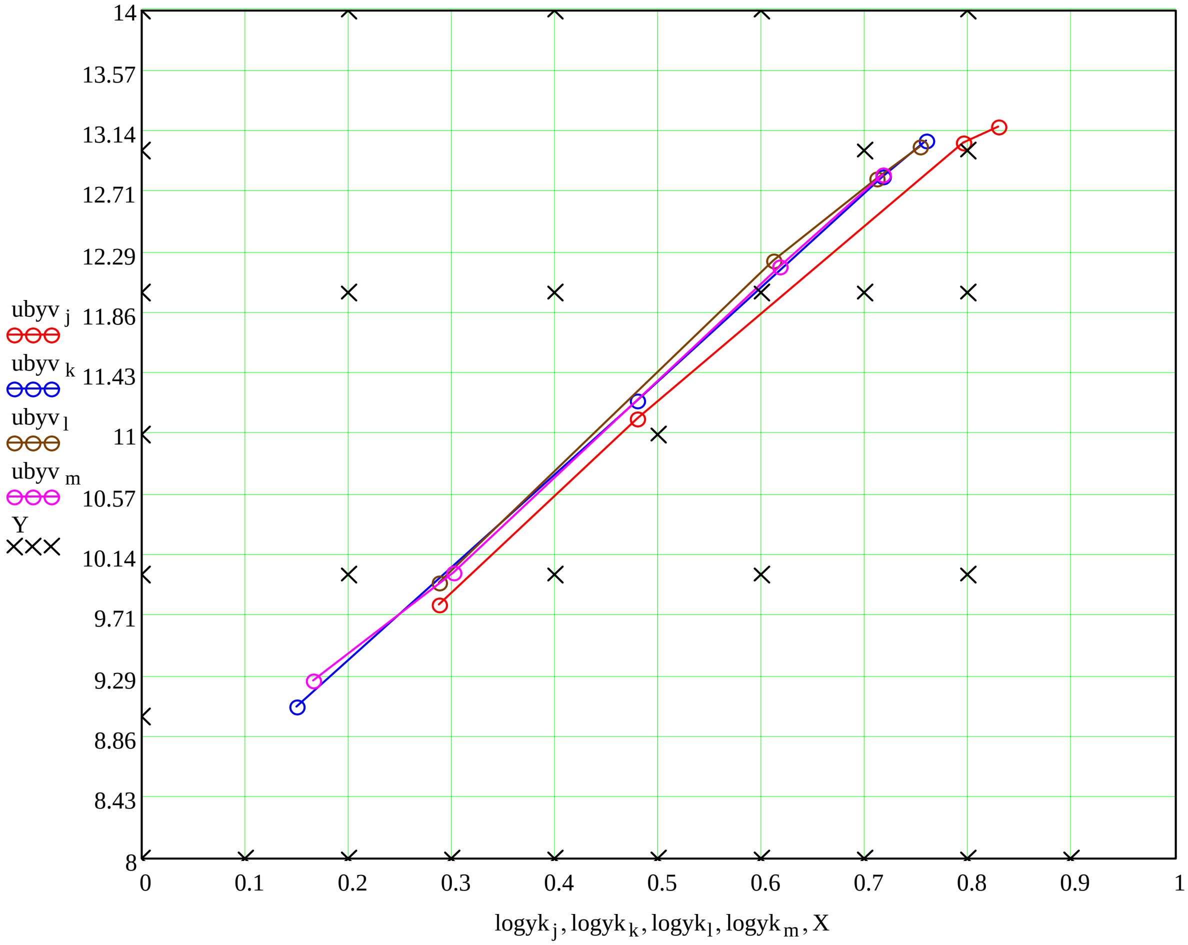

After obtaining the X and Y values, the distance from the wall and mean velocities were evaluated using following equations

$$k := 0.41 \cdot cm$$

$$y_i := k \cdot 10^{logyk_i}$$

	0
0	7.975
1	12.357
2	25.558
3	27.707
4	5.806
5	12.388
6	21.385
7	23.569
8	7.95
9	16.749
10	21.089
11	23.244
12	6.019
13	8.22
14	17.033
15	21.385

y = (table above) mm

$$V_r := \begin{pmatrix} 23.4 \\ 23.4 \\ 23.4 \\ 23.4 \\ 29.2 \\ 29.2 \\ 29.2 \\ 29.2 \\ 50.4 \\ 50.4 \\ 50.4 \\ 50.4 \\ 59.3 \\ 59.3 \\ 59.3 \\ 59.3 \end{pmatrix} \cdot \frac{cm}{sec}$$

$$u := \overrightarrow{\left(ubyv \cdot V_r\right)}$$

u =

	0
0	229.239
1	259.883
2	305.534
3	308.072
4	264.832
5	328.101
6	374.217
7	381.539
8	501.532
9	615.738
10	645.293
11	656.742
12	548.513
13	593.701
14	722.402
15	760.668

$\frac{cm}{sec}$

APPENDIX B

CALCULATING FRICTION VELOCITY

ORIGIN:= 1 (The origin was set to 1 cause MathCAD has default array starting from 0)

$$u := \begin{pmatrix} 229.239 \\ 259.883 \\ 305.534 \\ 308.072 \\ 264.832 \\ 328.101 \\ 374.217 \\ 381.539 \\ 501.532 \\ 615.743 \\ 645.293 \\ 656.742 \\ 548.513 \\ 593.701 \\ 722.402 \\ 760.668 \end{pmatrix} \cdot \frac{cm}{sec} \qquad y := \begin{pmatrix} 7.975 \\ 12.357 \\ 25.558 \\ 27.707 \\ 5.806 \\ 12.388 \\ 21.385 \\ 23.569 \\ 7.950 \\ 16.749 \\ 21.089 \\ 23.244 \\ 6.019 \\ 8.220 \\ 17.033 \\ 21.385 \end{pmatrix} \cdot mm$$

In order to find fiction velocity Equation (3.3) was used. Since the friction velocity is dependent on mean velocity U and diffrent for each profile, arrays like i,j,k and l are created for calculating friction velocity of each profile.

$\kappa := 0.4$ $\Delta y := 0 \cdot mm$

$i := 1..4$ $j := 5..8$ $k := 9..12$ $l := 13..16$

Calculating friction velocity:-

1) For U = 310 cm/sec

$u1 := 12.2 \cdot \frac{cm}{sec}$ $A1 := 176 \cdot \frac{cm}{sec^2}$

$w := 17 \cdot cm$ $b := 3.88cm$

$$u_{p1} := \sqrt{A1 \cdot b - \left(\frac{w + 2 \cdot b}{1.1 \cdot w}\right) \cdot u1^2}$$

$$u_{p1} = 22.041\frac{cm}{sec}$$

2) For U = 388 cm/sec

$u2 := 16.9 \cdot \frac{cm}{sec}$ $A2 := 267 \cdot \frac{cm}{sec^2}$

$$u_{p2} := \sqrt{A2 \cdot b - \left(\frac{w + 2 \cdot b}{1.1 \cdot w}\right) \cdot u2^2}$$

$$u_{p2} = 25.647\frac{cm}{sec}$$

3) For U = 668 cm/sec

$u3 := 27.7 \cdot \frac{cm}{sec}$ $A3 := 788 \cdot \frac{cm}{sec^2}$

$$u_{p3} := \sqrt{A3 \cdot b - \left(\frac{w + 2 \cdot b}{1.1 \cdot w}\right) \cdot u3^2}$$

$$u_{p3} = 45.183\frac{cm}{sec}$$

4) For U = 787 cm/sec

$$u4 := 32 \cdot \frac{cm}{sec} \qquad A4 := 1086 \cdot \frac{cm}{sec^2}$$

$$u_{p4} := \sqrt{A4 \cdot b - \left(\frac{w + 2 \cdot b}{1.1 \cdot w}\right) \cdot u4^2}$$

$$u_{p4} = 53.459 \frac{cm}{sec}$$

These are the values of the friction velocities for cone rougness, based on coleman's corrected friction velocity correlation.

APPENDIX C

CALCULATING THE WALL SHIFT (Δy) VALUES

For finding out the Wall shift values, equation 3.4 was used. For each profile the slope was equated to zero in order to get the optimum wall shift values.

Now for the calculation of the Δy values,

$M := 0 \qquad N := 4 \qquad u_{p1} = 22.041 \frac{cm}{sec}$

1) Given

$$M = \frac{N \cdot \left[\sum_{i=1}^{4} \left[(y-\Delta y)_i \cdot \left(\overrightarrow{\left[(y-\Delta y)\cdot \exp\left[-\left(\kappa \cdot \frac{u}{u_{p1}}\right)\right]\right]}\right)_i\right]\right] \ldots + 0 - \sum_{i=1}^{4} (y-\Delta y)_i \cdot \sum_{i=1}^{4} \left(\overrightarrow{\left[(y-\Delta y)\cdot \exp\left[-\left(\kappa \cdot \frac{u}{u_{p1}}\right)\right]\right]}\right)_i}{N \cdot \sum_{i=1}^{4} \left[(y-\Delta y)_i\right]^2 - \left[\sum_{i=1}^{4} (y-\Delta y)_i\right]^2}$$

$\Delta y_1 := \mathrm{Find}(\Delta y)$

$\Delta y_1 = 0.187\ cm$

2) Given

$$M = \frac{N \cdot \sum_{j=5}^{8} \left[(y_p-\Delta y)_j \cdot \left(\overrightarrow{\left[(y_p-\Delta y)\cdot \exp\left[-\left(\kappa \cdot \frac{u}{u_{p2}}\right)\right]\right]}\right)_j\right] - 0 \ldots + \sum_{j=5}^{8} (y_p-\Delta y)_j \cdot \sum_{j=5}^{8} \left(\overrightarrow{\left[(y_p-\Delta y)\cdot \exp\left[-\left(\kappa \cdot \frac{u}{u_{p2}}\right)\right]\right]}\right)_j}{N \cdot \sum_{j=5}^{8} \left[(y_p-\Delta y)_j\right]^2 - \left[\sum_{j=5}^{8} (y_p-\Delta y)_j\right]^2}$$

$\Delta y_2 := \mathrm{Find}(\Delta y)$

$\Delta y_2 := 0.247cm$

3) Given

$$M = \frac{N \cdot \sum_{k=9}^{12} \left[(y - \Delta y)_k \cdot \left(\overrightarrow{\left[(y - \Delta y) \cdot \exp\left[-\left(\kappa \cdot \frac{u}{u_{p3}} \right) \right] \right]} \right)_k \right] - 0 \ldots + \sum_{k=9}^{12} (y - \Delta y)_k \cdot \sum_{k=9}^{12} \left(\overrightarrow{\left[(y - \Delta y) \cdot \exp\left[-\left(\kappa \cdot \frac{u}{u_{p3}} \right) \right] \right]} \right)_k}{N \cdot \sum_{k=9}^{12} \left[(y - \Delta y)_k \right]^2 - \left[\sum_{k=9}^{12} (y - \Delta y)_k \right]^2}$$

$\Delta y_3 := \mathrm{Find}(\Delta y)$

$\Delta y_3 := 0.279\,cm$

4) Given

$$M = \frac{N \cdot \sum_{l=13}^{16} \left[(y - \Delta y)_l \cdot \left(\overrightarrow{\left[(y - \Delta y) \cdot \exp\left[-\left(\kappa \cdot \frac{u}{u_{p4}} \right) \right] \right]} \right)_l \right] - 0 \ldots + \sum_{l=13}^{16} (y - \Delta y)_l \cdot \sum_{l=13}^{16} \left(\overrightarrow{\left[(y - \Delta y) \cdot \exp\left[-\left(\kappa \cdot \frac{u}{u_{p4}} \right) \right] \right]} \right)_l}{N \cdot \sum_{l=13}^{16} \left[(y - \Delta y)_l \right]^2 - \left[\sum_{l=13}^{16} (y - \Delta y)_l \right]^2}$$

$\Delta y_4 := \mathrm{Find}(\Delta y)$

$\Delta y_4 := 0.228\,cm$

Obtained wall shift values are for the XXV plate with cone roughness in Schilchting's experiment.

APPENDIX D

CALCULATING INTERCEPT ‘A’

After calculating all the parameters needed to obtain intercept 'A' equation 3.7 was used to evaluate intercept values. The following values of intercept is calculated for the cone roughness values.

Now calculating the Intercept:-

$u_1 := 22.041 \cdot \frac{cm}{sec}$ $\Delta y_1 := 0.187 \cdot cm$ $k := 0.375 \cdot cm$ $u_2 := 25.647 \cdot \frac{cm}{sec}$

$\Delta y_2 := 0.247 \cdot cm$ $\Delta y_3 := 0.279 \cdot cm$ $u_3 := 45.183 \cdot \frac{cm}{sec}$ $u_4 := 53.459 \cdot \frac{cm}{sec}$

$\Delta y_4 := 0.228 \cdot cm$ $m := 13..16$ $l := 9..12$

1) $$A_1 := \frac{u}{u_1} - 5.75 \cdot \log\left(\frac{y_p - \Delta y_1}{k}\right)$$

$A_{1_i} =$

9.184
9.223
9.259
9.158

2) $$A_2 := \frac{u}{u_2} - 5.75 \cdot \log\left(\frac{y_p - \Delta y_2}{k}\right)$$

$A_{2_j} =$

10.618
10.364
10.55
10.563

3) $$A_3 := \frac{u}{u_3} - 5.75 \cdot \log\left(\frac{y_p - \Delta y_3}{k}\right)$$

$A_{3_l} =$

10.303
10.346
10.323
10.299

4) $A_4 := \frac{u}{u_4} - 5.75 \cdot \log\left(\frac{y_p - \Delta y_4}{k}\right)$

$A_{4_m} =$

10.268
9.957
10.093
10.163

Now putting the Intercept values in one Table:-

$$A := \begin{pmatrix} 9.184 \\ 9.223 \\ 9.259 \\ 9.158 \\ 10.618 \\ 10.364 \\ 10.550 \\ 10.563 \\ 10.303 \\ 10.346 \\ 10.323 \\ 10.299 \\ 10.268 \\ 9.957 \\ 10.093 \\ 10.163 \end{pmatrix}$$

For each profile the slope is same, hence the intercept was avaraged for the plate. The avarage intercept calculation is shown below where the summation is devided by the total number of the points.

$$\frac{\sum A}{16} = 10.042$$

APPENDIX E

CALCULATING THE UNCERTAINTY OF VELOCITY

ORIGIN:= 1

$$u := \begin{pmatrix} 229.239 \\ 259.883 \\ 305.534 \\ 308.072 \\ 264.832 \\ 328.101 \\ 374.217 \\ 381.539 \\ 501.532 \\ 615.743 \\ 645.293 \\ 656.742 \\ 548.513 \\ 593.701 \\ 722.402 \\ 760.668 \end{pmatrix} \cdot \frac{cm}{sec} \qquad y_p := \begin{pmatrix} 7.975 \\ 12.357 \\ 25.558 \\ 27.707 \\ 5.806 \\ 12.388 \\ 21.385 \\ 23.569 \\ 7.950 \\ 16.749 \\ 21.089 \\ 23.244 \\ 6.019 \\ 8.220 \\ 17.033 \\ 21.385 \end{pmatrix} \cdot mm$$

(the matrix here shows the velocity and distance from the wall)

$$\Delta h := \frac{u^2}{2 \cdot g} \qquad U_{\Delta y} := \frac{1}{1000} \cdot in \qquad U_{\Delta h} := 0.01 \cdot in$$

$\Delta h =$ (cm)

	1
1	26.793
2	34.435
3	47.596
4	48.39
5	35.759
6	54.886
7	71.4
8	74.221
9	128.247
10	193.307
11	212.306
12	219.907
13	153.399
14	179.715
15	266.077
16	295.012

(The matrix here evaluates the diffrence in height for each profile points which is used in calculation of the uncertainty of velocity)

$$U_u := 0.5 \cdot (2 \cdot g \cdot \Delta h)^{-0.5} \cdot 2 \cdot g \cdot U_{\Delta h}$$

The following equation is used to obtain the uncertainty of velocity.

$$U_u := 0.5 \cdot (2 \cdot g \cdot \Delta h)^{-0.5} \cdot 2 \cdot g \cdot U_{\Delta h}$$

The uncertainty in the velocity is shown in the following matrix for each data points in the profile.

$U_u =$ (in $\frac{cm}{sec}$)

	1
1	0.109
2	0.096
3	0.082
4	0.081
5	0.094
6	0.076
7	0.067
8	0.065
9	0.05
10	0.04
11	0.039
12	0.038
13	0.045
14	0.042
15	0.034
16	0.033

APPENDIX F

CALCULATING THE UNCERTAINTY OF FRICTION VELOCITY

The equation 2.7 was used as the data reduction equation for finding out the uncertainty of the friction velocity. The calculation here is carried out for each individual profile

- **First Profile:-**

$$\frac{1}{\rho}\cdot\frac{dp}{dx} = g\cdot\frac{\Delta h}{\Delta x}$$

(The pressure diffrence term is transformed to get simpler form to use uncertainty assumptions)

$$\frac{1}{\rho}\cdot\frac{dp}{dx} = A1$$

(The A1 variable was taken for simplification)

$A1 := 176\frac{cm}{sec^2}$ $\quad b := 4cm$ $\quad w := 17cm$ $\quad x := 280cm$

$$\Delta h := \frac{A1\cdot x}{g}$$

$\Delta h = 50.252cm$ $\quad \Delta x := 280cm$

$U_{\Delta h} := 2mm$ $\quad U_{\Delta x} := 1mm$ (Assumed values)

$$U := \left[\left(\frac{U_{\Delta h}}{\Delta h}\right)^2 + \left(\frac{U_{\Delta x}}{\Delta x}\right)^2\right]^{0.5}$$

(This equation gives uncertainty in measured velocity values)

$$U = 3.996\times 10^{-3}$$

$$U_{PD1} := U\cdot A1$$

$$U_{PD1} = 0.703\frac{cm}{sec^2}$$

(This is the uncertainty in pressure diffrence term)

Now for finding out the uncertainty in the Roughness velocity we will take the data we know and will define some new variable just for the sake of ease in use of MathCAD

$U_{PD1} = 0.703\frac{cm}{sec^2}$ $U_b := 1mm$ $U_w := 1mm$ $U_{s1} := 12.2\frac{cm}{sec}$

$U_{Us1} := \frac{5}{100} \cdot U_{s1}$

Now lets take some diffrent notations for the use in MathCAD

$\frac{dU_{rc}}{d\left(\frac{1}{\rho} \cdot \frac{dp}{dx}\right)} = \theta 1$ $\frac{dU_{rc}}{db} = \theta 2$ (The diffrentiation terms are given symbols for the purpose of simplification)

$\frac{dU_{rc}}{dw} = \theta 3$ $\frac{dU_{rc}}{dU_s} = \theta 4$

Now evaluating these diffrentiation terms,

$$\theta 1 := \frac{1}{2}\left(b \cdot A1 - \frac{w + 2 \cdot b}{1.1 \cdot w} \cdot U_{s1}{}^2\right)^{\frac{-1}{2}} \cdot (b)$$

$$\theta 2 := \frac{1}{2}\left(b \cdot A1 - \frac{w + 2 \cdot b}{1.1 \cdot w} \cdot U_{s1}{}^2\right)^{\frac{-1}{2}} \cdot \left(A1 - \frac{2}{1.1 \cdot w} \cdot U_{s1}{}^2\right)$$

$$\theta 3 := \frac{1}{2}\left(b \cdot A1 - \frac{w + 2 \cdot b}{1.1 \cdot w} \cdot U_{s1}{}^2\right)^{\frac{-1}{2}} \cdot \left(\frac{2 \cdot b}{1.1 \cdot w^2} \cdot U_{s1}{}^2\right)$$

$$\theta 4 := \frac{1}{2}\left(b \cdot A1 - \frac{w + 2 \cdot b}{1.1 \cdot w} \cdot U_{s1}{}^2\right)^{\frac{-1}{2}} \cdot \left(-2\frac{w + 2 \cdot b}{1.1 \cdot w} \cdot U_{s1}\right)$$

Now finding the Roughness velocity Uncertainty for the first profile:-

$$U_{rc1} := \left[\left(\theta 1 \cdot U_{PD1}\right)^2 + \left(\theta 2 \cdot U_b\right)^2 + \left(\theta 3 \cdot U_w\right)^2 + \left(\theta 4 \cdot U_{Us1}\right)^2\right]^{\frac{1}{2}}$$

$$U_{rc1} = 0.572 \frac{cm}{sec}$$

(This gives the uncertainty in friction velocity for the first profile)

Now doing the similar type of calculations is carried out for all rest of the profiles. The calculation details are not repeated for all the other profiles.

- **Second Profile:-**

$$\frac{1}{\rho} \cdot \frac{dp}{dx} = g \cdot \frac{\Delta h}{\Delta x}$$

$$\frac{1}{\rho} \cdot \frac{dp}{dx} = A2$$

$$A2 := 267 \frac{cm}{sec^2}$$

$$\Delta h := \frac{A2 \cdot x}{g}$$

$$\Delta h = 76.234 cm$$

$$U := \left[\left(\frac{U_{\Delta h}}{\Delta h}\right)^2 + \left(\frac{U_{\Delta x}}{\Delta x}\right)^2\right]^{0.5}$$

$$U = 2.648 \times 10^{-3}$$

$$U_{PD2} := U \cdot A2$$

$$U_{PD2} = 0.707 \frac{cm}{2}$$

Now for finding out the uncertainty in the Roughness velocity we will take th
know and will define soem new variable just for the sake of ease in use of Ma

$$U_{PD2} = 0.707\frac{cm}{sec^2} \qquad U_{s2} := 16.9\frac{cm}{sec}$$

$$U_{Us2} := \frac{5}{100} \cdot U_{s2}$$

Now lets take some diffrent notations for the use in MathCAD

$$\frac{dU_{rc}}{d\left(\frac{1}{\rho} \cdot \frac{dp}{dx}\right)} = \theta1 \qquad \frac{dU_{rc}}{db} = \theta2$$

$$\frac{dU_{rc}}{dw} = \theta3 \qquad \frac{dU_{rc}}{dU_s} = \theta4$$

Now evaluating these parameters

$$\theta1 := \frac{1}{2}\left(b \cdot A2 - \frac{w + 2 \cdot b}{1.1 \cdot w} \cdot {U_{s2}}^2\right)^{\frac{-1}{2}} \cdot (b)$$

$$\theta2 := \frac{1}{2}\left(b \cdot A2 - \frac{w + 2 \cdot b}{1.1 \cdot w} \cdot {U_{s2}}^2\right)^{\frac{-1}{2}} \cdot \left(A2 - \frac{2}{1.1 \cdot w} \cdot {U_{s2}}^2\right)$$

$$\theta3 := \frac{1}{2}\left(b \cdot A2 - \frac{w + 2 \cdot b}{1.1 \cdot w} \cdot {U_{s2}}^2\right)^{\frac{-1}{2}} \cdot \left(\frac{2 \cdot b}{1.1 \cdot w^2} \cdot {U_{s2}}^2\right)$$

$$\theta4 := \frac{1}{2}\left(b \cdot A2 - \frac{w + 2 \cdot b}{1.1 \cdot w} \cdot {U_{s2}}^2\right)^{\frac{-1}{2}} \cdot \left(-2\frac{w + 2 \cdot b}{1.1 \cdot w} \cdot U_{s2}\right)$$

Now finding the Roughness velocity Uncertainty for the first profile:-

$$U_{rc2} := \left[\left(\theta1 \cdot U_{PD2}\right)^2 + \left(\theta2 \cdot U_b\right)^2 + \left(\theta3 \cdot U_w\right)^2 + \left(\theta4 \cdot U_{Us2}\right)^2\right]^{\frac{1}{2}}$$

$$U_{rc2} = 0.859\frac{cm}{sec}$$

- **Third Profile:-**

$$\frac{1}{\rho} \cdot \frac{dp}{dx} = g \cdot \frac{\Delta h}{\Delta x}$$

$$\frac{1}{\rho} \cdot \frac{dp}{dx} = A3$$

$$A3 := 788\frac{cm}{sec^2}$$

$$\Delta h := \frac{A3 \cdot x}{g}$$

$$\Delta h = 224.99cm$$

$$U := \left[\left(\frac{U_{\Delta h}}{\Delta h}\right)^2 + \left(\frac{U_{\Delta x}}{\Delta x}\right)^2\right]^{0.5}$$

$$U = 9.58 \times 10^{-4}$$

$$U_{PD3} := U \cdot A3$$

$$U_{PD3} = 0.755\frac{cm}{2}$$

Now for finding out the uncertainty in the Roughness velocity we will take the c
know and will define soem new variable just for the sake of ease in use of Math

$U_{PD3} = 0.755\frac{cm}{sec^2}$ $U_{s3} := 27.7\frac{cm}{sec}$

$U_{Us3} := \frac{5}{100} \cdot U_{s3}$

Now lets take some diffrent notations for the use in MathCAD

$\frac{dU_{rc}}{d\left(\frac{1}{\rho} \cdot \frac{dp}{dx}\right)} = \theta 1$ $\frac{dU_{rc}}{db} = \theta 2$

$\frac{dU_{rc}}{dw} = \theta 3$ $\frac{dU_{rc}}{dU_s} = \theta 4$

Now evaluating these parameters

$$\theta 1 := \frac{1}{2}\left(b \cdot A3 - \frac{w + 2 \cdot b}{1.1 \cdot w} \cdot U_{s3}^2\right)^{\frac{-1}{2}} \cdot (b)$$

$$\theta 2 := \frac{1}{2}\left(b \cdot A3 - \frac{w + 2 \cdot b}{1.1 \cdot w} \cdot U_{s3}^2\right)^{\frac{-1}{2}} \cdot \left(A3 - \frac{2}{1.1 \cdot w} \cdot U_{s3}^2\right)$$

$$\theta 3 := \frac{1}{2}\left(b \cdot A3 - \frac{w + 2 \cdot b}{1.1 \cdot w} \cdot U_{s3}^2\right)^{\frac{-1}{2}} \cdot \left(\frac{2 \cdot b}{1.1 \cdot w^2} \cdot U_{s3}^2\right)$$

$$\theta 4 := \frac{1}{2}\left(b \cdot A3 - \frac{w + 2 \cdot b}{1.1 \cdot w} \cdot U_{s3}^2\right)^{\frac{-1}{2}} \cdot \left(-2\frac{w + 2 \cdot b}{1.1 \cdot w} \cdot U_{s3}\right)$$

Now finding the Roughness velocity Uncertainty for the first profile:-

$$U_{rc3} := \left[\left(\theta1 \cdot U_{PD3}\right)^2 + \left(\theta2 \cdot U_b\right)^2 + \left(\theta3 \cdot U_w\right)^2 + \left(\theta4 \cdot U_{Us3}\right)^2\right]^{\frac{1}{2}}$$

$$U_{rc3} = 1.351 \frac{cm}{sec}$$

- **Fourth Profile:-**

$$\frac{1}{\rho} \cdot \frac{dp}{dx} = g \cdot \frac{\Delta h}{\Delta x}$$

$$\frac{1}{\rho} \cdot \frac{dp}{dx} = A4$$

$$A4 := 1086 \frac{cm}{sec^2}$$

$$\Delta h := \frac{A4 \cdot x}{g}$$

$$\Delta h = 310.075 cm$$

$$U := \left[\left(\frac{U_{\Delta h}}{\Delta h}\right)^2 + \left(\frac{U_{\Delta x}}{\Delta x}\right)^2\right]^{0.5}$$

$$U = 7.373 \times 10^{-4}$$

$$U_{PD4} := U \cdot A4$$

$$U_{PD4} = 0.801 \frac{cm}{sec^2}$$

Now for finding out the uncertainty in the Roughness velocity we will take the data we know and will define some new variable just for the sake of ease in use of MathCAD

$$U_{PD4} = 0.801 \frac{cm}{sec^2} \qquad U_{s4} := 32 \frac{cm}{sec}$$

$$U_{Us4} := \frac{5}{100} \cdot U_{s4}$$

Now lets take some diffrent notations for the use in MathCAD

$$\frac{dU_{rc}}{d\left(\frac{1}{\rho} \cdot \frac{dp}{dx}\right)} = \theta 1 \qquad \frac{dU_{rc}}{db} = \theta 2$$

$$\frac{dU_{rc}}{dw} = \theta 3 \qquad \frac{dU_{rc}}{dU_s} = \theta 4$$

Now evaluating these parameters

$$\theta 1 := \frac{1}{2}\left(b \cdot A4 - \frac{w + 2 \cdot b}{1.1 \cdot w} \cdot U_{s4}^{2}\right)^{\frac{-1}{2}} \cdot (b)$$

$$\theta 2 := \frac{1}{2}\left(b \cdot A4 - \frac{w + 2 \cdot b}{1.1 \cdot w} \cdot U_{s4}^{2}\right)^{\frac{-1}{2}} \cdot \left(A4 - \frac{2}{1.1 \cdot w} \cdot U_{s4}^{2}\right)$$

$$\theta 3 := \frac{1}{2}\left(b \cdot A4 - \frac{w + 2 \cdot b}{1.1 \cdot w} \cdot U_{s4}^{2}\right)^{\frac{-1}{2}} \cdot \left(\frac{2 \cdot b}{1.1 \cdot w^2} \cdot U_{s4}^{2}\right)$$

$$\theta 4 := \frac{1}{2}\left(b \cdot A4 - \frac{w + 2 \cdot b}{1.1 \cdot w} \cdot U_{s4}^{2}\right)^{\frac{-1}{2}} \cdot \left(-2 \frac{w + 2 \cdot b}{1.1 \cdot w} \cdot U_{s4}\right)$$

Now finding the Roughness velocity Uncertainty for the first profile:-

$$U_{rc4} := \left[\left(\theta1 \cdot U_{PD4}\right)^2 + \left(\theta2 \cdot U_b\right)^2 + \left(\theta3 \cdot U_w\right)^2 + \left(\theta4 \cdot U_{Us4}\right)^2\right]^{\frac{1}{2}}$$

$$U_{rc4} = 1.542\frac{cm}{sec}$$

This values are friction velocity uncertainty values for the cone roughness plate XXV in Schilchting's experimen.

APPENDIX G

CALCULATING THE UNCERTAINTY IN WALL SHIFT (Δy)

ORIGIN:= 1

- **For finding out the uncertainty in Z for Cone Roughness**

Wall shift is function of both velocity (u) and distance from the wall(y). And the matrix below shows the velocity and distance from the wall.

$$u := \begin{pmatrix} 229.239 \\ 259.883 \\ 305.534 \\ 308.072 \\ 264.832 \\ 328.101 \\ 374.217 \\ 381.539 \\ 501.532 \\ 615.743 \\ 645.293 \\ 656.742 \\ 548.513 \\ 593.701 \\ 722.402 \\ 760.668 \end{pmatrix} \cdot \frac{cm}{sec} \qquad U_u := \begin{pmatrix} 0.109 \\ 0.096 \\ 0.082 \\ 0.081 \\ 0.094 \\ 0.076 \\ 0.067 \\ 0.065 \\ 0.050 \\ 0.040 \\ 0.039 \\ 0.038 \\ 0.045 \\ 0.042 \\ 0.034 \\ 0.033 \end{pmatrix} \cdot \frac{cm}{sec} \qquad y := \begin{pmatrix} 07.975 \\ 12.357 \\ 25.558 \\ 27.707 \\ 05.806 \\ 12.388 \\ 21.385 \\ 23.569 \\ 07.950 \\ 16.749 \\ 21.089 \\ 23.244 \\ 06.019 \\ 08.220 \\ 17.033 \\ 21.385 \end{pmatrix} \cdot mm$$

$$U_y := \frac{1}{1000} \cdot in \qquad \Delta Y := \frac{U_u}{1000} \cdot sec \qquad u_{p1} := 22.041 \cdot \frac{cm}{sec}$$

$$M := 0 \qquad N := 4 \qquad \kappa := 0.4 \qquad \Delta X := \frac{U_y}{1000}$$

$$\Delta y := 1mm \qquad U_{up1} := 0.572 \cdot \frac{cm}{sec}$$

In order to get the components of data reduction equation. Each of the points in above given matrix was added uncertainty separately each time and the diffrence in wall shift was calculated.

Given

$$M = \frac{N \cdot \sum_{i=1}^{4} \left[(y - \Delta y)_i \cdot \left(\overrightarrow{\left[(y - \Delta y) \cdot \exp\left[-\left(\kappa \cdot \frac{u}{u_{p1}} \right) \right] \right]} \right)_i \right] - \ldots + \sum_{i=1}^{4} (y - \Delta y)_i \cdot \sum_{i=1}^{4} \left(\overrightarrow{\left[(y - \Delta y) \cdot \exp\left[-\left(\kappa \cdot \frac{u}{u_{p1}} \right) \right] \right]} \right)_i}{N \cdot \sum_{i=1}^{4} \left[(y - \Delta y)_i \right]^2 - \left[\sum_{i=1}^{4} (y - \Delta y)_i \right]^2}$$

$\Delta y_1 := \mathrm{Find}(\Delta y)$

$\Delta y_1 := 0.187\,cm$

Each time the value in one of the matrix was added it's individual uncertainty and the change in wall shift was calculated. The following values are for the first profile only.

- Creating the database for the wall shift values by changing X & Y coordinates :

- For the first profile

$f := 0.186972\,cm$

$fx1 := 0.186975\,cm$	$fy1 := 0.186971\,cm$
$fx2 := 0.186973\,cm$	$fy2 := 0.186971\,cm$
$fx3 := 0.186972\,cm$	$fy3 := 0.186973\,cm$
$fx4 := 0.186971\,cm$	$fy4 := 0.186973\,cm$

After getting the different wall shift values, the basic diffrentiation formula was use to get the terms for the data re duction equation.

Now for calculating the terms in the data reduction equation

$$\theta1 := \frac{fx1 - f}{\Delta X} \qquad \theta5 := \frac{fy1 - f}{\Delta Y_1}$$

$$\theta2 := \frac{fx2 - f}{\Delta X} \qquad \theta6 := \frac{fy2 - f}{\Delta Y_2}$$

$$\theta3 := \frac{fx3 - f}{\Delta X} \qquad \theta7 := \frac{fy3 - f}{\Delta Y_3}$$

$$\theta4 := \frac{fx4 - f}{\Delta X} \qquad \theta8 := \frac{fy4 - f}{\Delta Y_4}$$

- Now for finding the Uncertainty in wall shift:-

$$U_{z1} := \left[\theta1^2 \cdot U_y^2 + \theta2^2 \cdot U_y^2 + \theta3^2 \cdot U_y^2 + \theta4^2 \cdot U_y^2 + \theta5^2 \cdot \left(U_{u_1} \cdot sec\right)^2 \ldots \\ + \theta6^2 \cdot \left(U_{u_2} \cdot sec\right)^2 + \theta7^2 \cdot \left(U_{u_3} \cdot sec\right)^2 + \theta8^2 \cdot \left(U_{u_4} \cdot sec\right)^2\right]^{0.5}$$

$U_{z1} = 0.039mm$

Now doing the similar kind of calculations for all the profiles we will get the Uncertainty values for the wall Shift which is tabulated as below.

$$U_z := \begin{pmatrix} 0.03873 \\ 0.034641 \\ 0.031623 \\ 0.026458 \end{pmatrix} mm$$

APPENDIX H

CALCULATING THE UNCERTAINTY OF INTERCEPT, $\frac{k_s}{k}$ AND $\frac{k_s}{k_{eff}}$

After evaluationg uncertainties in each paramenter of equation 3.12, uncertainty in the intercept a was obtained by using equation 3.12 as the data reduction equation.

$$A = \frac{u}{u_{rc}} - 5.75\log\left(\frac{y - \Delta y}{k}\right) \qquad \text{..........(i)}$$

Now for this eq.(i), we have following data.

$$u := \begin{pmatrix} 229.239 \\ 259.883 \\ 305.534 \\ 308.072 \\ 264.832 \\ 328.101 \\ 374.217 \\ 381.539 \\ 501.532 \\ 615.743 \\ 645.293 \\ 656.742 \\ 548.513 \\ 593.701 \\ 722.402 \\ 760.668 \end{pmatrix} \cdot \frac{cm}{sec} \quad U_u := \begin{pmatrix} 0.109 \\ 0.096 \\ 0.082 \\ 0.081 \\ 0.094 \\ 0.076 \\ 0.067 \\ 0.065 \\ 0.050 \\ 0.040 \\ 0.039 \\ 0.038 \\ 0.045 \\ 0.042 \\ 0.034 \\ 0.033 \end{pmatrix} \frac{cm}{sec} \quad u_{rc} := \begin{pmatrix} 22.041 \\ 22.041 \\ 22.041 \\ 22.041 \\ 25.647 \\ 25.647 \\ 25.647 \\ 25.647 \\ 45.183 \\ 45.183 \\ 45.183 \\ 45.183 \\ 53.459 \\ 53.459 \\ 53.459 \\ 53.459 \end{pmatrix} \frac{cm}{sec} \quad U_{urc} := \begin{pmatrix} 0.572 \\ 0.572 \\ 0.572 \\ 0.572 \\ 0.859 \\ 0.859 \\ 0.859 \\ 0.859 \\ 1.351 \\ 1.351 \\ 1.351 \\ 1.351 \\ 1.542 \\ 1.542 \\ 1.542 \\ 1.542 \end{pmatrix} \frac{cm}{sec}$$

$$U_y := \frac{1}{1000} in$$

$$y := \begin{pmatrix} 7.975 \\ 12.357 \\ 25.558 \\ 27.707 \\ 5.806 \\ 12.388 \\ 21.385 \\ 23.569 \\ 7.950 \\ 16.749 \\ 21.089 \\ 23.244 \\ 6.019 \\ 8.220 \\ 17.033 \\ 21.385 \end{pmatrix} \cdot mm \qquad \Delta y := \begin{pmatrix} 0.187 \\ 0.187 \\ 0.187 \\ 0.187 \\ 0.247 \\ 0.247 \\ 0.247 \\ 0.247 \\ 0.279 \\ 0.279 \\ 0.279 \\ 0.279 \\ 0.228 \\ 0.228 \\ 0.228 \\ 0.228 \end{pmatrix} cm \qquad U_{\Delta y} := \begin{pmatrix} 0.03873 \\ 0.03873 \\ 0.03873 \\ 0.03873 \\ 0.034641 \\ 0.034641 \\ 0.034641 \\ 0.034641 \\ 0.031623 \\ 0.031623 \\ 0.031623 \\ 0.031623 \\ 0.026458 \\ 0.026458 \\ 0.026458 \\ 0.026458 \end{pmatrix} mm \qquad A := \begin{pmatrix} 9.184 \\ 9.223 \\ 9.259 \\ 9.158 \\ 10.618 \\ 10.364 \\ 10.550 \\ 10.563 \\ 10.303 \\ 10.346 \\ 10.323 \\ 10.299 \\ 10.268 \\ 9.957 \\ 10.093 \\ 10.163 \end{pmatrix}$$

The diffrentiation terms used to find out intercept uncertainty is given simple notations in order to ease the calculation in MathCAD

$$\frac{dA}{du} = \theta 1 \qquad \theta 1 := \frac{1}{u_{rc}}$$

$$\frac{dA}{du_{rc}} = \theta 2 \qquad \theta 2 := \frac{-u}{u_{rc}^{2}}$$

$$\frac{dA}{dy} = \theta 3 \qquad \theta 3 := \frac{-5.75}{(y - \Delta y) \cdot \ln(10)}$$

$$\frac{dA}{d(\Delta y)} = \theta 4 \qquad \theta 4 := \frac{5.75}{(y - \Delta y) \cdot \ln(10)}$$

The following is to find out the uncertainty in intercept A, all the tems are kno
equation

$$U_A := \overrightarrow{\left[\theta1^2 \cdot U_u^{\ 2} + \theta2^2 \cdot U_{urc}^{\ 2} + \theta3^2 \cdot \left(U_y^{\ 2}\right) + \theta4^2 \cdot U_{\Delta y}^{\ 2}\right]^{\frac{1}{2}}}$$

$U_A =$

	0
0	0.271
1	0.306
2	0.36
3	0.363
4	0.347
5	0.429
6	0.489
7	0.498
8	0.332
9	0.408
10	0.427
11	0.435
12	0.297
13	0.321
14	0.39
15	0.41

Now for finding the uncertainty in the Avg. value of intercept 'A'

$$\overline{A}_{XXV} = \frac{A_1 + A_2 + \ldots + A_N}{N} \qquad N := 16$$

- using the above equation as the data reduction equation and finding the u
  avg. value of A for the first profile

$$U_{Aavg} := \left[\left(\frac{U_{A_0}}{N}\right)^2 + \left(\frac{U_{A_1}}{N}\right)^2 + \left(\frac{U_{A_2}}{N}\right)^2 + \left(\frac{U_{A_3}}{N}\right)^2 + \left(\frac{U_{A_4}}{N}\right)^2 + \left(\frac{U_{A_5}}{N}\right)^2 \ldots + \left(\frac{U_{A_6}}{N}\right)^2 + \left(\frac{U_{A_7}}{N}\right)^2 + \left(\frac{U_{A_8}}{N}\right)^2 + \left(\frac{U_{A_9}}{N}\right)^2 + \left(\frac{U_{A_{10}}}{N}\right)^2 + \left(\frac{U_{A_{11}}}{N}\right)^2 \ldots + \left(\frac{U_{A_{12}}}{N}\right)^2 + \left(\frac{U_{A_{13}}}{N}\right)^2 + \left(\frac{U_{A_{14}}}{N}\right)^2 + \left(\frac{U_{A_{15}}}{N}\right)^2\right]^{\frac{1}{2}}$$

$U_{Aavg} = 0.096$

Now in the next step we will find out the ks/k for each of these profile

for simplicity, assuming $\frac{k_s}{k} = B$

For the first profile

$A_{avg} := 10.042$ (The avarage intercept values that are calculated earlier)

$$B := 10^{\frac{8.48 - A_{avg}}{5.75}}$$

$B = 0.535$

Hence,

Now the Uncertainty in this ks/k, (B)

$$U_{ksbyk} := \left[\left[(-0.174) \cdot 10^{1.475 - 0.174 \cdot A_{avg}} \cdot \ln(10) \cdot U_{Aavg} \right]^2 \right]^{\frac{1}{2}}$$

$U_{ksbyk} = 0.021$

Now in the next step we will find out the ks/keff for each of these profiles

for simplicity, assuming $\frac{k_s}{k_{eff}} = C$ $k_{eff} := 0.357226573 \cdot cm$ $k := 0.375 \cdot cm$

$$C := \frac{k}{k_{eff}} (B)$$

$$C = 0.562$$

Hence,

Now the Uncertainty in this ks/keff, (C)

$$U_{ksbykeff} := \left[\left[\left(\frac{k}{k_{eff}} \right) \cdot U_{ksbyk} \right]^2 \right]^{\frac{1}{2}}$$

$$U_{ksbykeff} = 0.022$$

APPENDIX I

RESULTS

The following matrix A is data calculated for the diffrnt surfaces used in schichting's study. The second matrix is the uncertainties in the equivalent sand grain roughness height for the corresponding plates.

$$A := \begin{pmatrix} 2.721351731 & 21.30969176 \\ 2.664523218 & 22.32842909 \\ 3.918238151 & 27.20346969 \\ 6.856309717 & 30.35615025 \\ 1.872774352 & 40.35792649 \\ 1.983041818 & 69.71072537 \\ 0.44016369 & 85.64881671 \\ 0.494434103 & 89.02297675 \\ 0.419224721 & 89.9384882 \\ 0.611338744 & 110.5553881 \\ 0.611101363 & 114.344459 \\ 0.299465918 & 125.2563251 \\ 0.124625205 & 190.7937644 \\ 0.035118818 & 258.7032585 \\ 0.046551588 & 333.5576343 \\ 0.120663779 & 364.8094111 \\ 0.018328449 & 446.7639769 \end{pmatrix} \qquad U_{ks} := \begin{pmatrix} 0.10718 \\ 0.06872 \\ 0.0000 \\ 0.06924 \\ 0.07016 \\ 0.109330 \\ 0.02812 \\ 0.0200 \\ 0.02369 \\ 0.0000 \\ 0.0000 \\ 0.00211 \\ 0.01200 \\ 0.00467 \\ 0.00616 \\ 0.00926 \\ 0.03366 \end{pmatrix}$$

The following notations explains the components in the matrix. The graph on the next page shows the data poins and it's uncertainties.

$$\frac{d}{dx}\log(x) \rightarrow \frac{1}{x \cdot \ln(10)}$$

$$k_s := A^{\langle 0 \rangle} \qquad \Lambda_s := A^{\langle 1 \rangle}$$

$$NN := \text{rows}(k_s) - 1 \qquad m := 0..\,NN$$

$$Y := \log(k_s) \qquad X := \log(\Lambda_s)$$

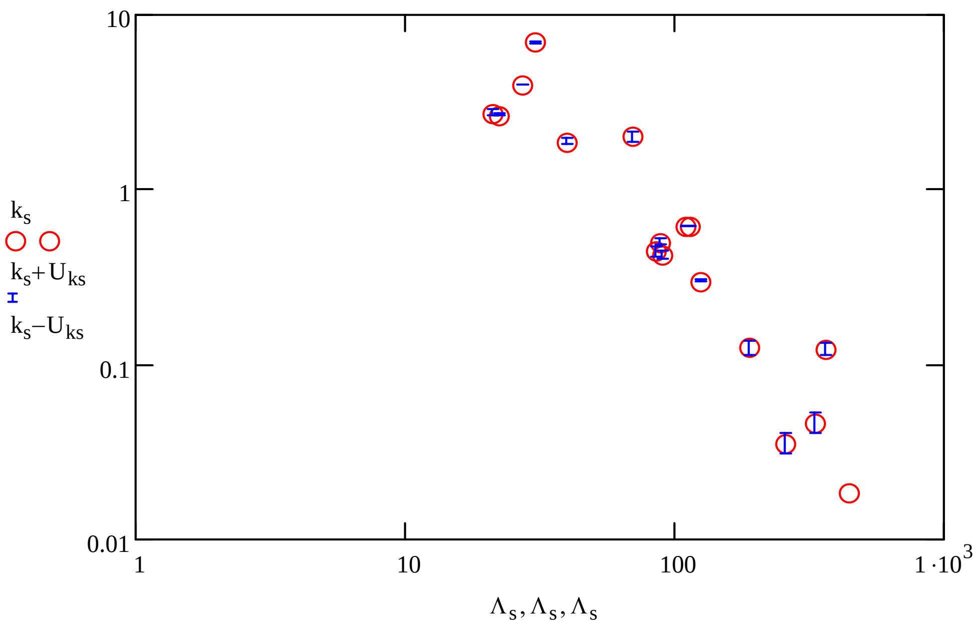

$N := \text{rows}(X) \qquad i := 0..\, N-1$

The calibration range must first be set. The calibration range is taken to be the range of x values in the data points plus 25% on each side.

$j := 0..\, 150$

$$L_j := \min(\Lambda_s) + j \cdot \frac{\max(\Lambda_s) - \min(\Lambda_s)}{150}$$

The uncertainties in the measurement of x are shown below.

$P_L := 0.0 \qquad B_L := 0.0$

If the x values are measured using the same instruments as were used in the calibration data enter "1" in the correlation coefficient definition below. Otherwise, enter "0".

$\rho_{xX} := 0$

$$m := \frac{N \cdot \sum_{j=0}^{N-1} (X_j \cdot Y_j) - \sum_{j=0}^{N-1} X_j \cdot \sum_{j=0}^{N-1} Y_j}{N \cdot \sum_{j=0}^{N-1} (X_j)^2 - \left(\sum_{j=0}^{N-1} X_j\right)^2} \qquad m = -1.669$$

Check:

$\text{slope}(X, Y) = -1.669$

$$b := \frac{\sum_{j=0}^{N-1} (X_j)^2 \cdot \sum_{j=0}^{N-1} Y_j - \sum_{j=0}^{N-1} X_j \cdot \sum_{j=0}^{N-1} (X_j \cdot Y_j)}{N \cdot \sum_{j=0}^{N-1} (X_j)^2 - \left(\sum_{j=0}^{N-1} X_j\right)^2} \qquad b = 2.967$$

Check:

$\text{intercept}(X, Y) = 2.967$

The data reduction equation for the calibration curve is shown below.

$$\frac{k_s}{k_{eff}} = 10^b \Lambda_{eff}^{\ m} \qquad \text{or} \qquad K = 10^b \cdot L^m$$

$$\frac{k_s}{k_{eff}}(\Lambda_{eff}, k, \Lambda) = K(\Lambda_{eff}, k, \Lambda) = 10^{b(X(\Lambda), Y(k))} L^{m(X(\Lambda), Y(k))}$$

Expressed completely in terms of transformed variables, the DRE is shown below.

$$K = 10^{\frac{\sum_{j=0}^{N-1} (X_j)^2 \cdot \sum_{j=0}^{N-1} Y_j - \sum_{j=0}^{N-1} X_j \cdot \sum_{j=0}^{N-1} (X_j \cdot Y_j)}{N \cdot \sum_{j=0}^{N-1} (X_j)^2 - \left(\sum_{j=0}^{N-1} X_j\right)^2}} \cdot L^{\frac{N \cdot \sum_{j=0}^{N-1} (X_j \cdot Y_j) - \sum_{j=0}^{N-1} X_j \cdot \sum_{j=0}^{N-1} Y_j}{N \cdot \sum_{j=0}^{N-1} (X_j)^2 - \left(\sum_{j=0}^{N-1} X_j\right)^2}}$$

where,

$X = \log(\Lambda_{eff})$ and $Y = \log\left(\frac{k_s}{k_{eff}}\right)$

The partial derivaties are now calculated for each measured variable. To make the expressions simpler,the derivatives with respect to m and b will be found first.

$$\frac{dK}{dk} = \frac{dK}{db} \cdot \frac{db}{dY} \cdot \frac{dY}{dk} + \frac{dK}{dm} \cdot \frac{dm}{dY} \cdot \frac{dY}{dk} = \theta Kb \cdot \theta bY \cdot \theta Yk + \theta Km \cdot \theta mY \cdot \theta Yk$$

$$\theta Kb_{i,j} := 10^b (L_j)^m \cdot \ln(10) \qquad \theta Km_{i,j} := 10^b (L_j)^m \cdot \ln(L_j)$$

$$\theta mY_i := \frac{N \cdot X_i - \sum_{j=0}^{N-1} X_j}{N \cdot \sum_{j=0}^{N-1} (X_j)^2 - \left(\sum_{j=0}^{N-1} X_j\right)^2} \qquad \theta bY_i := \frac{\sum_{j=0}^{N-1} (X_j)^2 - X_i \cdot \sum_{j=0}^{N-1} X_j}{N \cdot \sum_{j=0}^{N-1} (X_j)^2 - \left(\sum_{j=0}^{N-1} X_j\right)^2}$$

$$\theta Yk_i := \frac{1}{k_{s_i} \cdot \ln(10)}$$

$$\log(K) = b + m \cdot \log(L)$$

$$\frac{d}{dx} 10^x \rightarrow 10^x \cdot \ln(10)$$

$$Ynew = \log(K)$$

Then the overall partial derivatives with respect to the calibration curve are shown below.

$$\theta Kk_{i,j} := \theta Kb_{i,j} \cdot \theta bY_i \cdot \theta Yk_i + \theta Km_{i,j} \cdot \theta mY_i \cdot \theta Yk_i$$

$$\theta KY_j := 10^{b+m \cdot \log(L_j)} \cdot \ln(10)$$

The standard estimate of the error is calculated below and added as a random uncertainty.

$$S_Y := \left[\frac{\sum_{i=0}^{N-1} \left(Y_i - m \cdot X_i - b\right)^2}{N-2}\right]^{0.5} \qquad S_Y = 0.258$$

$$K_j := 10^b \cdot \left(L_j\right)^m$$

$$U_j := \left[\sum_{k=0}^{N-1} \left(\theta Kk_{k,j} \cdot U_{ks_k}\right)^2 + \left(2 \cdot S_Y\right)^2 \cdot \left(\theta KY_j\right)^2\right]^{0.5}$$

However, the above equation is based on the assumption that the uncertainties are small and that the first order approximations of the derivatives are sufficient to describe the behavior of the data reduction equation. This is definitely not the case for the uncertainty caused by the standare error of the estimate for the regression. For this case, the data reduction equation is highly non-linear, the uncertainty is NOT small, and the first order derivatives are not sufficient.

For the standard error of the estimate part, the

$$UL_j := \left[\sum_{k=0}^{N-1} \left(\theta Kk_{k,j} \cdot U_{ks_k}\right)^2 + \left(K_j - 10^{\log(K_j) - 2 \cdot S_Y}\right)^2\right]^{0.5}$$

$$UU_j := \left[\sum_{k=0}^{N-1} \left(\theta Kk_{k,j} \cdot U_{ks_k}\right)^2 + \left(K_j - 10^{\log(K_j) + 2 \cdot S_Y}\right)^2\right]^{0.5}$$

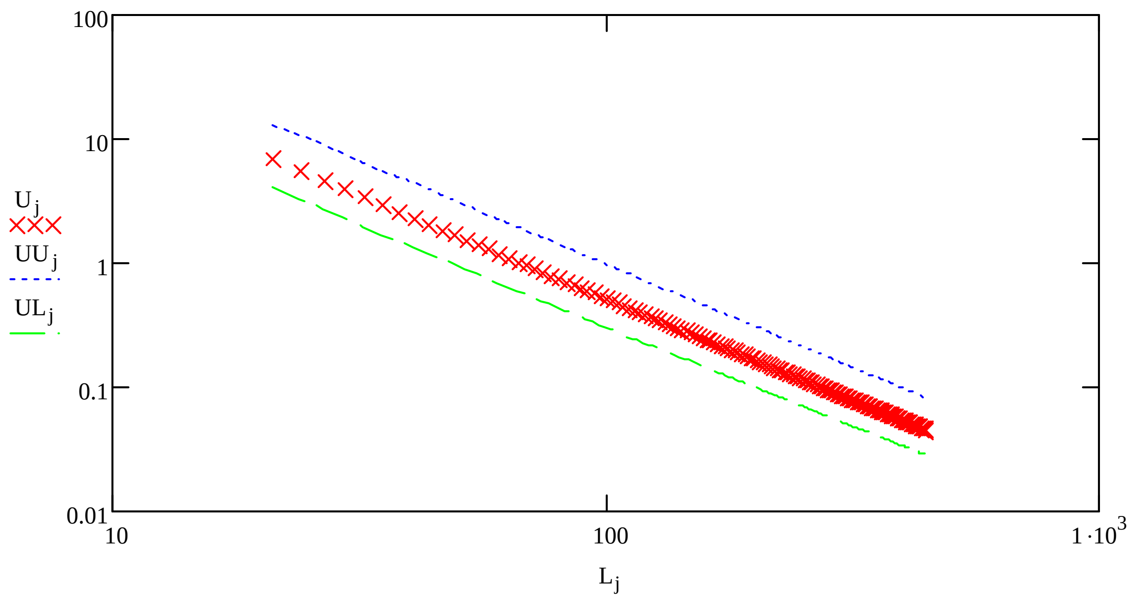
100
10
1
0.1
0.01
10
100
1·10^3
U_j
UU_j
UL_j
L_j

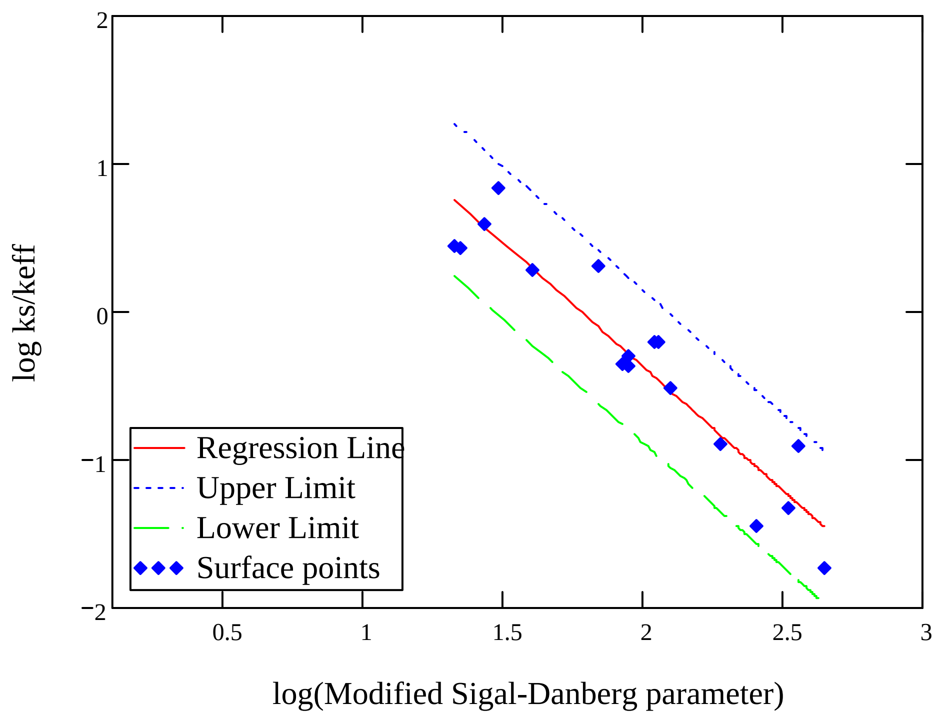
2
1
0
−1
−2
0.5
1
1.5
2
2.5
3
log ks/keff
log(Modified Sigal-Danberg parameter)
Regression Line
Upper Limit
Lower Limit
Surface points

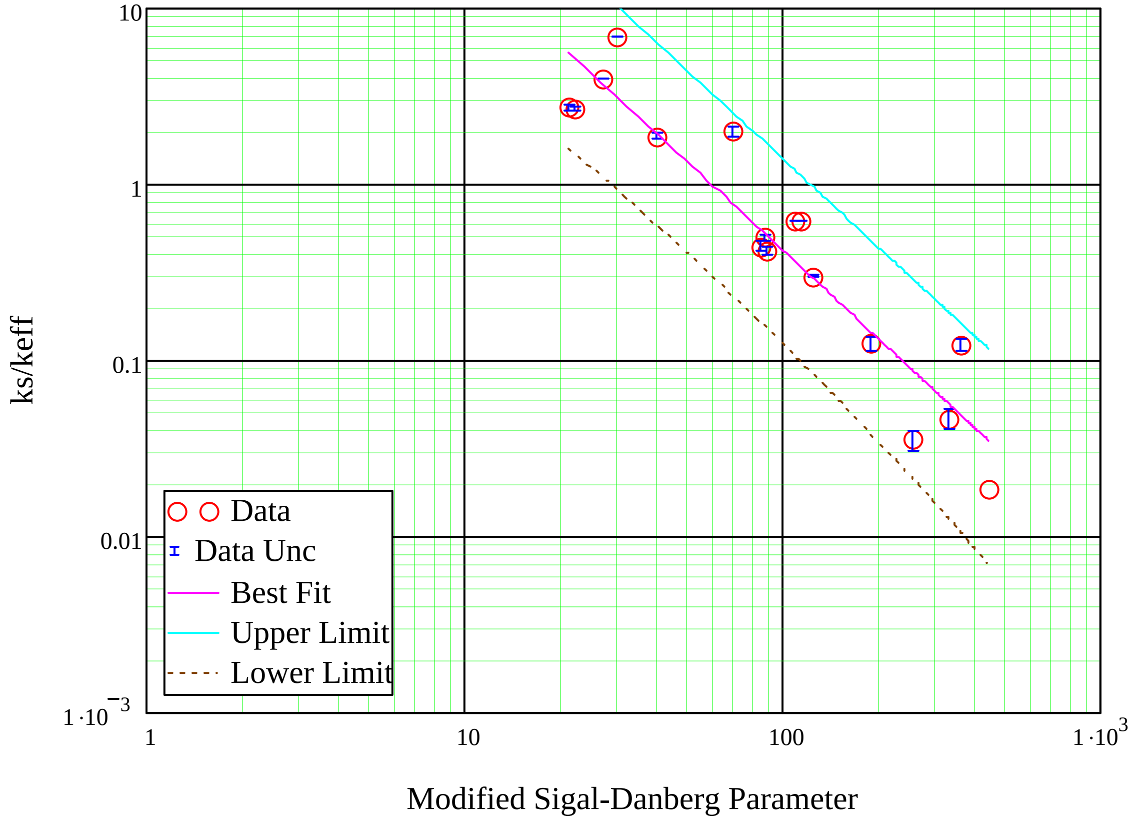
10
1
0.1
0.01
$1 \cdot 10^{-3}$
1
10
100
$1 \cdot 10^{3}$
ks/keff
Modified Sigal-Danberg Parameter
Data
Data Unc
Best Fit
Upper Limit
Lower Limit

APPENDIX J

SKIN FRICTION COEFFICIENT SAMPLE CALCULATION

This worksheet provides an example prediction of skin friction coefficient for a deterministic surface using the modified Sigal-Danberg correlation for equivalent sand-grain roughness height. The surface used for the example calculation is surface No. XXV of Schlichting which is comprised of truncated cones. The geometry of surface No. XXV is entered below:

$k_{eff} := 0.35722 \cdot cm$ — k_{eff} is the maximum height of the surface above the mean surface elevation.

$\Lambda_{eff} := 89.023$ — Λ_{eff} is the Sigal-Danberg parameter based on the surface features above the mean elevation.

The predicted ratio of the equivalent sandgrain roughness height to the effective roughness heigh (ks/keff)corr is found using the correlation of McClain et al [Ref.]

$$\left(\frac{k_s}{k_{eff}}\right) = R_{corr} = 927.317 \cdot \Lambda_{eff}^{-1.669}$$

The predicted height ratio is then:

$R_{corr} := 927.317 \cdot \Lambda_{eff}^{-1.669}$

$R_{corr} = 0.517$

R_{corr} is the ratio of the equivalent sandgrain roughness height to the effective roughness height predicted by the correlation of McClain et al. [13].

The uncertainty in the predicted height ratio is found from Appendix I. In Appendix I, the uncertainty in the predicted height ratio is split into a positive uncertainty and a negative uncertainty. Both are entered below (U_{Rpos} and U_{Rneg}).

$U_{Rpos} := 1.175$

$U_{Rneg} := 0.361$

The equivalent sandgrain roughness value for surface No. XXV is then evaluated as:

$k_s := k_{eff} \cdot R_{corr}$ $\quad$ $k_s = 0.185\,cm$

If the measurement of the effective roughness height is assumed to be perfect, then the positive and negative uncertainties in the predicted equivalent sandgrain roughness height are then:

$U_{kspos} := k_{eff} \cdot U_{Rpos}$ $\quad$ $U_{kspos} = 0.42\,cm$

$U_{ksneg} := k_{eff} \cdot U_{Rneg}$ $\quad$ $U_{ksneg} = 0.129\,cm$

The intent of calculating an effective sand grain roughness height is to use that value for predicting skin friction coefficients using a corrlation such as that of White [15] for zero-pressure gradient, turbulent flow over a flat plate.

$$C_f = \left(1.4 + 3.7 \cdot \log\left(\frac{x}{k_s}\right)\right)^{-2}$$

To explore the expected uncertainties in skin friction coefficient predictions, example conditions must be assumed. The example calculations are made for a 20 m/s flow of air over a flat plate. The properties of air and the velocity of the airflow are entered for the calculation.

$\rho_{air} := 1.17 \cdot \frac{kg}{m^3}$ — ρ_{air} is the density of air at 25 C and 1 atm.

$\mu_{air} := 18.4 \cdot 10^{-6} \cdot \frac{N \cdot s}{m^2}$ — μ_{air} is the molecular viscosity of air at 25 C and 1 atm.

$U_e := 20 \cdot \frac{m}{s}$ — U_e is the assumed velocity of the air over a flat plate.

Flow over a flat plat naturally transitions to turbulent flow at Reynolds numbers about 250,000. For the predictive demonstration, a Reynolds number 1,000,000 is used.

$$Re_x := 1 \cdot 10^6$$

The distance from the flat-plate's knife-edge is then calculated from the Reynold's number definition.

$$x := \frac{Re_x \cdot \mu_{air}}{\rho_{air} \cdot U_e} \qquad x = 0.786\,m$$

White's expression can now be used to predict a skin friction coefficient.

$$C_f := \left(1.4 + 3.7 \cdot \log\left(\frac{x}{k_s}\right)\right)^{-2} \qquad \boxed{C_f = 0.00808}$$

The uncertainty of the predicted skin friction coefficient based on the uncertainty from the equivalent sandgrain roughness height (neglecting the correlation uncertainty itself) is then evaluated using

$$U_{Cf} = \left(\frac{d}{dk_s} Cf\right) \cdot U_{ks}$$

The derivative of the skin friction coefficient with respect to the equivalent sandgrain roughness height, θ_{ks}, is evaluated next.

$$\theta_{ks} := \frac{7.4}{\left(1.4 + 3.7 \cdot \frac{\ln\left(\frac{x}{k_s}\right)}{\ln(10)}\right)^3 \cdot k_s \cdot \ln(10)}$$

Since the equivalent sandgrain roughness height has positive and negative uncertainty skin friction coefficient uncertainty calculation must also
be split. The positive and negative uncertiainty limits are calculated separately.

$U_{Cfpos} := \theta_{ks} \cdot U_{kspos}$ $\quad U_{Cfpos} = 0.0053$

$U_{Cfneg} := \theta_{ks} \cdot U_{ksneg}$ $\quad U_{Cfneg} = 0.00163$

Using the calcualted uncertainties, the upper and lower limits on the skin friction coefficient are then determined as

$C_f + U_{Cfpos} = 0.01338$

$C_f - U_{Cfneg} = 0.00645$

The percentage uncertainties (upper and lower) are determined:

$\frac{U_{Cfpos}}{C_f} = 65.635\%$ $\quad \frac{U_{Cfneg}}{C_f} = 20.165\%$

Hence, for the sample surface (Schlichting's surface No. XXV), the predicted skin friction coefficient for 20 m/s flow of air over a flat plate with Reynolds number 10^6 is 0.00808. However, based only on the uncertainty in the predicted equivalent sand-grain roughness value from the modified Sigal-Danberg correlation, the actual value may be as high as 0.01338 (65.63%) or as low as 0.00645 (20.16%) with alevel of confidence of 95%